Can Class-Priors Help Single-Positive Multi-Label Learning?

Biao Liu, Ning Xu*, Jie Wang, Xin Geng
School of Computer Science and Engineering, Southeast University,
Nanjing 210096, China
Key Laboratory of New Generation Artificial Intelligence Technology and
Its Interdisciplinary Applications (Southeast University),
Ministry of Education, China
*Corresponding author: xning@seu.edu.cn

Abstract

Single-positive multi-label learning (SPMLL) is a weakly supervised multi-label learning problem, where each training example is annotated with only one positive label. Existing SPMLL methods typically assign pseudo-labels to unannotated labels with the assumption that prior probabilities of all classes are identical. However, the class-prior of each category may differ significantly in real-world scenarios, which makes the predictive model not perform as well as expected due to the unrealistic assumption on real-world application. To alleviate this issue, a novel framework named CRISP, i.e., Class-pRiors Induced Single-Positive multi-label learning, is proposed. Specifically, a class-priors estimator is introduced, which can estimate the class-priors that are theoretically guaranteed to converge to the ground-truth class-priors. In addition, based on the estimated class-priors, an unbiased risk estimator for classification is derived, and the corresponding risk minimizer can be guaranteed to approximately converge to the optimal risk minimizer on fully supervised data. Experimental results on ten MLL benchmark datasets demonstrate the effectiveness and superiority of our method over existing SPMLL approaches.

1 Introduction

Multi-label learning (MLL) is a learning paradigm that aims to train a model on examples associated with multiple labels to accurately predict relevant labels for unknown instances [43, 25]. Over the past decade, MLL has been successfully applied to various real-world applications, including image annotation [30], text classification [24], and facial expression recognition [2].

Compared with multi-class-single-label learning, where each example is associated with a unique label, MLL involves instances that are assigned multiple labels. As the number of examples or categories is large, accurately annotating each label of an example becomes exceedingly challenging. To address the high annotation cost, single-positive multi-label learning (SPMLL) has been proposed [5, 38], where each training example is annotated with only one positive label. Moreover, since many examples in multi-class datasets, such as ImageNet [42], contain multiple categories but are annotated with a single label, employing SPMLL allows for the derivation of multi-label predictors from existing numerous multi-class datasets, thereby expanding the applicability of MLL.

To address the issue that model tends to predict all labels as positive if trained with only positive labels, existing SPMLL methods typically assign pseudo-labels to unannotated labels. Cole et al. updates the pseudo-labels as learnable parameters with a regularization to constrain the number of expected positive labels [5]. Xu et al. recovers latent soft pseudo-labels by employing variational label enhancement [38]. Zhou et al. adopts asymmetric-tolerance strategies to update pseudo-labels

39th Conference on Neural Information Processing Systems (NeurIPS 2025).

cooperating with an entropy-maximization loss [45]. Xie et al. utilizes contrastive learning to learn the manifold structure information and updates the pseudo-labels with a threshold [33].

These approaches rely on a crucial assumption that prior probabilities of all classes are identical. However, in real-world scenarios, the class-prior of each category may differ significantly. This unrealistic assumption will introduce severe biases into the pseudo-labels, further impacting the training of the model supervised by the inaccurate pseudo-labels. As a result, the learned model could not perform as well as expected.

Motivated by the above consideration, we propose a novel framework named CRISP, i.e., Class-pRiors Induced Single-Positive multi-label learning. Specifically, a class-priors estimator is derived, which determines an optimal threshold by estimating the ratio between the fraction of positive labeled samples and the total number of samples receiving scores above the threshold. The estimated class-priors can be theoretically guaranteed to converge to the ground-truth class-priors. In addition, based on the estimated class-priors, an unbiased risk estimator for classification is derived, which guarantees the learning consistency [26] and ensures that the obtained risk minimizer would approximately converge to the optimal risk minimizer on fully supervised data. Our contributions can be summarized as follows:

- Practically, for the first time, we propose a novel framework for SPMLL named CRISP, which estimates the class-priors and then an unbiased risk estimator is derived based on the estimated class-priors, addressing the unrealistic assumption of identical class-priors for all classes.
- Theoretically, the estimated class-priors can be guaranteed to converge to the ground-truth class-priors. Additionally, we prove that the risk minimizer corresponding to the proposed risk estimator can be guaranteed to approximately converge to the optimal risk minimizer on fully supervised data.

Experiments on four multi-label image classification (MLIC) datasets and six MLL datasets show the effectiveness of our methods over several existing SPMLL approaches.

2 Related Work

Multi-label learning is a supervised machine learning technique where an instance is associated with multiple labels simultaneously. The study of label correlations in multi-label learning has been extensive, and these correlations can be categorized into first-order, second-order, and high-order correlations. First-order correlations involve adapting binary classification algorithms for multi-label learning, such as treating each label as an independent binary classification problem [1, 27]. Second-order correlations model pairwise relationships between labels [7, 9]. High-order correlations take into account the relationships among multiple labels, such as employing graph convolutional neural networks to extract correlation information among all label nodes [3]. Furthermore, there has been an increasing interest in utilizing label-specific features, which are tailored to capture the attributes of a specific label and enhance the performance of the models [41, 11].

In practice, accurately annotating each label for every instance in multi-label learning is unfeasible due to the immense scale of the output space. Consequently, multi-label learning with missing labels (MLML) has been introduced [28]. MLML methods primarily rely on low-rank, embedding, and graph-based models. The presence of label correlations implies a low-rank output space [25], which has been extensively employed to fill in the missing entries in a label matrix [35, 40, 34]. Another widespread approach is based on embedding techniques that map label vectors to a low-dimensional space, where features and labels are jointly embedded to exploit the complementarity between the feature and label spaces [39, 31]. Additionally, graph-based models are prevalent solutions for MLML, constructing a label-specific graph for each label from a feature-induced similarity graph and incorporating manifold regularization into the empirical risk minimization framework [28, 32].

In SPMLL, a specific case of multi-label learning with incomplete labels, only one of the multiple positive labels is observed. The initial work treats all unannotated labels as negative and updates the pseudo-labels as learnable parameters, applying a regularization to constrain the number of expected positive labels [5]. A label enhancement process [37, 22, 21, 36, 16] is used to recover latent soft labels and train the multi-label classifier [38]. The introduction of an asymmetric pseudo-label approach utilizes asymmetric-tolerance strategies for pseudo-labels, along with an entropy-maximization loss

[45]. Additionally, Xie et al. proposes a label-aware global consistency regularization method, leveraging the manifold structure information learned from contrastive learning to update pseudo-labels [33]. Liu et al. investigates the theoretical guarantee of pseudo-label-based methods for SPMLL [23], proving the learnability of such methods and proposing a mutual label enhancement approach that iteratively refines the label distributions [15, 17, 19, 18, 14] of samples and optimizes the multi-label classifier.

3 Preliminaries

3.1 Multi-Label Learning

Let $\mathcal{X} = \mathbb{R}^q$ denote the instance space and $\mathcal{Y} = \{0, 1\}^c$ denote the label space with c classes. Given the MLL training set $\mathcal{D} = \{(\boldsymbol{x}_i, \boldsymbol{y}_i)|1 \leq i \leq n\}$ where $\boldsymbol{x}_i \in \mathcal{X}$ is a q-dimensional instance and $\boldsymbol{y}_i \in \mathcal{Y}$ is its corresponding labels. Here, $\boldsymbol{y}_i = [y_i^1, y_i^2, \ldots, y_i^c]$ where $y_i^j = 1$ indicates that the j-th label is a relevant label associated with $\boldsymbol{x}_i$ and $y_i^j = 0$ indicates that the j-th label is irrelevant to $\boldsymbol{x}_i$. Multi-label learning is intended to produce a multi-label classifier in the hypothesis space $h \in \mathcal{H} : \mathcal{X} \mapsto \mathcal{Y}$ that minimizes the following classification risk:

$$\mathcal{R}(h) = \mathbb{E}_{(\boldsymbol{x},\boldsymbol{y})\sim p(\boldsymbol{x},\boldsymbol{y})} \left[\mathcal{L}(h(\boldsymbol{x}), \boldsymbol{y})\right], \tag{1}$$

where $\mathcal{L} : \mathcal{X} \times \mathcal{Y} \mapsto \mathbb{R}^+$ is a multi-label loss function that measures the accuracy of the model in fitting the data. Note that a method is risk-consistent if the method possesses a classification risk estimator that is equivalent to $\mathcal{R}(f)$ given the same classifier [26].

3.2 Single-Positive Multi-Label Learning

For single-positive multi-label learning (SPMLL), each instance is annotated with only one positive label. Given the SPMLL training set $\tilde{\mathcal{D}} = \{(\boldsymbol{x}_i, \gamma_i)|1 \leq i \leq n\}$ where $\gamma_i \in \{1, 2, \ldots, c\}$ denotes the only observed single positive label of $\boldsymbol{x}_i$. For each SPMLL training example $(\boldsymbol{x}_i, \gamma_i)$, we use the observed single-positive label vector $\boldsymbol{l}_i = [l_i^1, l_i^2, \ldots, l_i^c]^\top \in \{0, 1\}^c$ to represent whether j-th label is the observed positive label, i.e., $l_i^j = 1$ if $j = \gamma_i$, otherwise $l_i^j = 0$. The task of SPMLL is to induce a multi-label classifier $h \in \mathcal{H} : \mathcal{X} \mapsto \mathcal{Y}$ from $\tilde{\mathcal{D}}$, which can assign the unknown instance with a set of relevant labels.

4 The Proposed Method

4.1 The CRISP Algorithm

In this section, we introduce our novel framework, CRISP, i.e., Class-pRiors Induced Single-Positive multi-label learning. This framework alternates between estimating class-priors and optimizing an unbiased risk estimator under the guidance of the estimated class-priors.

Firstly, we introduce the class-priors estimator for SPMLL, leveraging the blackbox classifier f to estimate the class-prior of each label. The class-priors estimator exploits the classifier f to give each input a score, indicating the likelihood of it belonging to a positive sample of j-th label. Specifically, the class-priors estimator determines an optimal threshold by estimating the ratio between the fraction of the total number of samples and that of positive labeled samples receiving scores above the threshold, thereby obtaining the class-prior probability of the j-th label.

Motivated by the definition of top bin in learning from positive and unlabeled data (PU learning) [10], for a given probability density function $p(\boldsymbol{x})$ and a classifier f, define the threshold cumulative density function $q_j(z) = \int_{S_z} p(\boldsymbol{x})d\boldsymbol{x}$ where $S_z = \{\boldsymbol{x} \in \mathcal{X} : f^j(\boldsymbol{x}) \geq z\}$ for all $z \in [0, 1]$. $q_j(z)$ captures the cumulative density of the feature points which are assigned a value larger than a threshold z by the classifier of the j-th label. We now define an empirical estimator of $q_j(z)$ as $\hat{q}_j(z) = \frac{1}{n}\sum_{i=1}^{n} \mathbf{1}(f^j(\boldsymbol{x}_i) \geq z)$ where $\mathbf{1}(\cdot)$ is the indicator function. For each probability density function $p_j^p = p(\boldsymbol{x}|y_j = 1)$, $p_j^n = p(\boldsymbol{x}|y_j = 0)$ and $p = p(\boldsymbol{x})$, we define $q_j^p = \int_{S_z} p(\boldsymbol{x}|y_j = 1)d\boldsymbol{x}$ and $q_j^n = \int_{S_z} p(\boldsymbol{x}|y_j = 0)d\boldsymbol{x}$ respectively.

Algorithm 1 CRISP Algorithm

Input: The SPMLL training set $\tilde{\mathcal{D}} = \{(\boldsymbol{x}_i, \gamma_i) | 1 \leq i \leq n\}$, the multi-label classifier f, the number of epoch T, hyperparameters $0 \leq \delta, \tau \leq 1$;

1: **for** $t = 1$ **to** T **do**
2: **for** $j = 1$ **to** c **do**
3: Extract the positive-labeled samples set $\mathcal{S}_{L_j} = \{\boldsymbol{x}_i : l_i^j = 1, 1 \leq i \leq n\}$.
4: Estimate $\hat{q}_j(z) = \frac{1}{n}\sum_{i=1}^{n} \mathbf{1}(f^j(\boldsymbol{x}_i) \geq z)$ and $\hat{q}_j^p(z) = \frac{1}{n_j^p}\sum_{\boldsymbol{x}\in\mathcal{S}_{L_j}} \mathbf{1}(f^j(\boldsymbol{x}) \geq z)$ for all $z \in [0, 1]$.
5: Estimate the class-prior of j-th label by $\hat{\pi}_j = \frac{\hat{q}_j(\hat{z})}{\hat{q}_j^p(\hat{z})}$ with the threshold induced by Eq. (2).
6: **end for**
7: Update the model f by forward computation and back-propagation by Eq. (7) using the estimated class-priors.
8: **end for**

Output: The predictive model f.

The steps involved in the procedure are as follows: Firstly, for each label, we extract a positive-labeled samples set $\mathcal{S}_{L_j} = \{\boldsymbol{x}_i : l_i^j = 1, 1 \leq i \leq n\}$ from the entire dataset. Next, with $\mathcal{S}_{L_j}$, we estimate the fraction of the total number of samples that receive scores above the threshold $\hat{q}_j(z) = \frac{1}{n}\sum_{i=1}^{n} \mathbf{1}(f^j(\boldsymbol{x}_i) \geq z)$ and that of positive labeled samples receiving scores above the threshold $\hat{q}_j^p(z) = \frac{1}{n_j^p}\sum_{\boldsymbol{x}\in\mathcal{S}_{L_j}} \mathbf{1}(f^j(\boldsymbol{x}) \geq z)$ for all $z \in [0, 1]$, where $n_j^p = |\mathcal{S}_{L_j}|$ is the cardinality of the positive-labeled samples set of j-th label. Finally, the class-prior of j-th label is estimated by $\frac{\hat{q}_j(\hat{z})}{\hat{q}_j^p(\hat{z})}$ at $\hat{z}$ that minimizes the upper confidence bound defined in Theorem 4.1.

Theorem 4.1. *Define* $z^\star = \arg\min_{z\in[0,1]} q_j^n(z)/q_j^p(z)$*, for every* $0 < \delta < 1$*, define* $\hat{z} = \arg\min_{z\in[0,1]} \left(\frac{\hat{q}_j(z)}{\hat{q}_j^p(z)} + \frac{1+\tau}{\hat{q}_j^p(z)}\left(\sqrt{\frac{\log(4/\delta)}{2n}} + \sqrt{\frac{\log(4/\delta)}{2n_j^p}}\right)\right)$*. Assume* $n_j^p \geq 2\frac{\log 4/\delta}{q_j^p(z^\star)}$*, the estimated class-prior* $\hat{\pi}_j = \frac{\hat{q}_j(\hat{z})}{\hat{q}_j^p(\hat{z})}$ *satisfies with probability at least* $1 - \delta$*:*

$$\pi_j - \frac{c_1}{q_j^p(z^\star)}\left(\sqrt{\frac{\log(4/\delta)}{2n}} + \sqrt{\frac{\log(4/\delta)}{2n_p}}\right) \leq \hat{\pi}_j \leq \pi_j + (1-\pi_j)\frac{q_j^n(z^\star)}{q_j^p(z^\star)} + \frac{c_2}{q_j^p(z^\star)}\left(\sqrt{\frac{\log(4/\delta)}{2n}} + \sqrt{\frac{\log(4/\delta)}{2n_p}}\right),$$

where $c_1, c_2 \geq 0$ are constants and τ is a fixed parameter ranging in $(0, 1)$. The proof can be found in Appendix A.1. Theorem 4.1 provides a principle for finding the optimal threshold. Under the condition that the threshold $\hat{z}$ satisfies:

$$\hat{z} = \arg\min_{z\in[0,1]} \left(\frac{\hat{q}_j(z)}{\hat{q}_j^p(z)} + \frac{1+\tau}{\hat{q}_j^p(z)}\left(\sqrt{\frac{\log(4/\delta)}{2n}} + \sqrt{\frac{\log(4/\delta)}{2n_j^p}}\right)\right), \tag{2}$$

the estimated class-prior $\hat{\pi}_j$ of j-th category will converge to the ground-truth class-prior with enough training samples. Practically, to determine the optimal threshold in Eq. (2), we conduct an exhaustive search across the set of outputs generated by the function f^j for each class. The details can be found in Appendix A.2.

After obtaining an accurate estimate of class-prior for each category, we proceed to utilize these estimates as a form of supervision to guide the training of our model. Firstly, the classification risk $\mathcal{R}(f)$ on fully supervised information can be written as [1]:

$$\mathcal{R}(f) = \mathbb{E}_{(\boldsymbol{x},\boldsymbol{y})\sim p(\boldsymbol{x},\boldsymbol{y})}\left[\mathcal{L}(f(\boldsymbol{x}), \boldsymbol{y})\right] = \sum_{\boldsymbol{y}} p(\boldsymbol{y})\mathbb{E}_{\boldsymbol{x}\sim p(\boldsymbol{x}|\boldsymbol{y})}\left[\mathcal{L}(f(\boldsymbol{x}), \boldsymbol{y})\right]. \tag{3}$$

[1]The datail is provided in Appendix A.3.

In Eq. (3), the loss function $\mathcal{L}(f(\boldsymbol{x}), \boldsymbol{y})$ is calculated for each label separately, which is a commonly used approach in multi-label learning:

$$\mathcal{L}(f(\boldsymbol{x}), \boldsymbol{y}) = \sum_{j=1}^{c} y_j \ell(f^j(\boldsymbol{x}), 1) + (1 - y_j)\ell(f^j(\boldsymbol{x}), 0). \tag{4}$$

By substituting Eq. (4) into Eq. (3), the classification risk $\mathcal{R}(f)$ can be written as follows with the absolute loss function[2]:

$$\mathcal{R}(f) = \sum_{j=1}^{c} 2p(y_j = 1)\mathbb{E}_{\boldsymbol{x}\sim p(\boldsymbol{x}|y_j=1)}\left[1 - f^j(\boldsymbol{x})\right] + \left(\mathbb{E}_{\boldsymbol{x}\sim p(\boldsymbol{x})}\left[f^j(\boldsymbol{x})\right] - p(y_j = 1)\right). \tag{5}$$

The rewritten classification risk comprises two distinct components. The first component computes the risk solely for the positively labeled samples, and the second component leverages the unlabeled data to estimate difference between the expected output of the model f and the class-prior $\pi_j = p(y_j = 1)$ to align the expected class-prior outputted by model with the ground-truth class-prior.

During the training process, the prediction of model can be unstable due to insufficiently labeled data. This instability may cause a large divergence between the expected class-prior $\mathbb{E}[f^j(\boldsymbol{x})]$ and the ground-truth class-prior π_j, even leading to a situation where the difference between $\mathbb{E}[f^j(\boldsymbol{x})]$ and π_j turns negative [44]. To ensure non-negativity of the classification risk and the alignment of class-priors, absolute function is added to the second term. Then the risk estimator can be written as:

$$\mathcal{R}_{sp}(f) = \sum_{j=1}^{c} 2\pi_j \mathbb{E}_{\boldsymbol{x}\sim p(\boldsymbol{x}|y_j=1)}\left[1 - f^j(\boldsymbol{x})\right] + \left|\mathbb{E}_{\boldsymbol{x}\sim p(\boldsymbol{x})}\left[f^j(\boldsymbol{x})\right] - \pi_j\right|. \tag{6}$$

Therefore, we could express the empirical risk estimator via:

$$\widehat{\mathcal{R}}_{sp}(f) = \sum_{j=1}^{c} \frac{2\pi_j}{|\mathcal{S}_{L_j}|} \sum_{\boldsymbol{x}\in\mathcal{S}_{L_j}} \left(1 - f^j(\boldsymbol{x})\right) + \left|\frac{1}{n}\sum_{\boldsymbol{x}\in\tilde{\mathcal{D}}} \left(f^j(\boldsymbol{x}) - \pi_j\right)\right|. \tag{7}$$

The proposed equation enables the decomposition of the risk over the entire dataset into terms that can be estimated using both labeled positive and unlabeled samples.

In MLL datasets, where the number of negative samples for each label significantly exceeds that of positive samples, there is a tendency for the decision boundary to be biased towards the center of positive samples, especially for rare classes. This bias is further exacerbated in SPMLL due to the common strategy of assuming unobserved labels as negative [5, 38, 33] to warm up the model. To alleviate the issue, we propose a modification of Eq. (7):

$$\widehat{\mathcal{R}}_{sp}(f) = \sum_{j=1}^{c} \frac{2\pi_j}{|\mathcal{S}_{L_j}|} \sum_{\boldsymbol{x}\in\mathcal{S}_{L_j}} \left(1 - \frac{1}{1 + e^{-(g^j(\boldsymbol{x}) + \lambda\pi^j)}}\right) + \left|\frac{1}{n}\sum_{\boldsymbol{x}\in\tilde{\mathcal{D}}} \left(f^j(\boldsymbol{x}) - \pi_j\right)\right|. \tag{8}$$

where λ is a hyper-parameter and $g^j(\boldsymbol{x})$ represents the logit of j-th label outputted by the network for instance $\boldsymbol{x}$ and $f^j(\boldsymbol{x}) = \sigma(g^j(\boldsymbol{x}))$ where $\sigma(\cdot)$ denotes the sigmoid function.

The algorithmic description of CRISP is shown in Algorithm 1.

4.2 Estimation Error Bound

In this subsection, an estimation error bound is established for Eq. (7) to demonstrate its learning consistency. Firstly, we define the function spaces as:

$$\mathcal{G}_{sp}^{L} = \left\{(\boldsymbol{x}, \boldsymbol{l}) \mapsto \sum_{j=1}^{c} 2\pi_j l_j \left(1 - f^j(\boldsymbol{x})\right) | f \in \mathcal{F}\right\}, \mathcal{G}_{sp}^{U} = \left\{(\boldsymbol{x}, \boldsymbol{l}) \mapsto \sum_{j=1}^{c} \left(f^j(\boldsymbol{x}) - \pi_j\right) | f \in \mathcal{F}\right\},$$

and denote the expected Rademacher complexity [26] of the function spaces as:

$$\widetilde{\mathfrak{R}}_n\left(\mathcal{G}_{sp}^{L}\right) = \mathbb{E}_{\boldsymbol{x},y,\boldsymbol{\sigma}}\left[\sup_{g\in\mathcal{G}_{sp}^{L}} \sum_{i=1}^{n} \sigma_i g\left(\boldsymbol{x}_i, y_i\right)\right], \widetilde{\mathfrak{R}}_n\left(\mathcal{G}_{sp}^{U}\right) \quad = \mathbb{E}_{\boldsymbol{x},\boldsymbol{y},\boldsymbol{\sigma}}\left[\sup_{g\in\mathcal{G}_{sp}^{U}} \sum_{i=1}^{n} \sigma_i g\left(\boldsymbol{x}_i, \boldsymbol{y}_i\right)\right],$$

Table 1: Predictive performance of each comparing method on four MLIC datasets in terms of *mean average precision (mAP)* (mean ± std). The best performance is highlighted in bold (the larger the better).

	VOC	COCO	NUS	CUB
AN	85.546±0.294	64.326±0.204	42.494±0.338	18.656±0.090
AN-LS	87.548±0.137	67.074±0.196	43.616±0.342	16.446±0.269
WAN	87.138±0.240	65.552±0.171	45.785±0.192	14.622±1.300
EPR	85.228±0.444	63.604±0.249	45.240±0.338	19.842±0.423
ROLE	88.088±0.167	67.022±0.141	41.949±0.205	14.798±0.613
EM	88.674±0.077	70.636±0.094	47.254±0.297	20.692±0.527
EM-APL	88.860±0.080	70.758±0.215	47.778±0.181	21.202±0.792
SMILE	87.314±0.150	70.431±0.213	47.241±0.172	18.611±0.144
PLC	88.021±0.121	70.422±0.062	46.211±0.155	**21.840±0.237**
LL-R	87.784±0.063	70.078±0.008	48.048±0.074	18.966±0.022
LL-CP	87.466±0.031	70.460±0.032	48.000±0.077	19.310±0.164
LL-CT	87.054±0.214	70.384±0.058	47.930±0.010	19.012±0.097
BOOSTLU+LL-R	89.224±0.017	73.272±0.006	49.590±0.021	19.136±0.009
BOOSTLU+LL-CP	88.358±0.212	70.820±0.030	47.810±0.166	18.166±0.063
BOOSTLU+LL-CT	88.528±0.053	71.742±0.006	48.216±0.021	17.952±0.007
CRISP	**89.820±0.191**	**74.640±0.219**	**49.996±0.316**	21.650±0.178

where $\boldsymbol{\sigma} = \{\sigma_1, \sigma_2, \cdots, \sigma_n\}$ is n Rademacher variables with σ_i independently uniform variable taking value in $\{+1, -1\}$. Then we have:

Theorem 4.2. *Assume the loss function* $\mathcal{L}_{sp}^{L} = \sum_{j=1}^{c} 2\pi_j l_j \left(1 - f^j(\boldsymbol{x})\right)$ *and* $\mathcal{L}_{sp}^{U} = \sum_{j=1}^{c} \left(f^j(\boldsymbol{x}) - \pi_j\right)$ *could be bounded by* M*, i.e.,* $M = \sup_{\boldsymbol{x}\in\mathcal{X}, f\in\mathcal{F}, \boldsymbol{y}\in\mathcal{Y}} \max(\mathcal{L}_{sp}^{L}(f(\boldsymbol{x}), \boldsymbol{y}), \mathcal{L}_{sp}^{U}(f(\boldsymbol{x}), \boldsymbol{y}))$*, with probability at least* $1-\delta$*, we have:*

$$\mathcal{R}(\hat{f}_{sp}) - \mathcal{R}(f^\star) \leq \frac{4\sqrt{2}\rho}{C} \sum_{j=1}^{c} \mathfrak{R}_n(\mathcal{H}_j) + \frac{M}{\min_j |\mathcal{S}_{L_j}|} \sqrt{\frac{\log \frac{4}{\delta}}{2n}} + 4\sqrt{2} \sum_{j=1}^{c} \mathfrak{R}_n(\mathcal{H}_j) + M\sqrt{\frac{\log \frac{4}{\delta}}{2n}}.$$

where C is a constant, $\hat{f}_{sp} = \min_{f\in\mathcal{F}} \widehat{\mathcal{R}}_{sp}(f)$, $f^\star = \min_{f\in\mathcal{F}} \mathcal{R}(f)$ are the empirical risk minimizer and the true risk minimizer respectively and $\rho = \max_j 2\pi_j$, $\mathcal{H}_j = \left\{h : \boldsymbol{x} \mapsto f^j(\boldsymbol{x}) | f \in \mathcal{F}\right\}$ and $\mathfrak{R}_n\left(\mathcal{H}_j\right) = \mathbb{E}_{p(\boldsymbol{x})}\mathbb{E}_{\boldsymbol{\sigma}}\left[\sup_{h\in\mathcal{H}_j} \frac{1}{n} \sum_{i=1}^{n} h\left(\boldsymbol{x}_i\right)\right]$. The proof can be found in Appendix A.5.

Theorem 4.2 shows that, as $n \to \infty$, $\hat{f}_{sp}$ would converge to $f^\star$ with an intrinsic error quantified by the Rademacher complexity terms, reflecting the complexity of the hypothesis space. Note that the error is a fundamental aspect of the learning problem and remains even in a fully supervised scenario [26].

5 Experiments

5.1 Experimental Configurations

Datasets. In the experimental section, our proposed method is evaluated on four large-scale multi-label image classification (MLIC) datasets and six widely-used multi-label learning (MLL) datasets. The four MLIC datasets include `PSACAL VOC 2021 (VOC)` [8], `MS-COCO 2014 (COCO)` [20], `NUS-WIDE (NUS)` [4], and `CUB-200 2011 (CUB)` [29]; the MLL datasets cover a wide range of scenarios with heterogeneous multi-label characteristics. For each MLIC dataset, 20% of the training set is withheld for validation. Each MLL dataset is partitioned into train/validation/test sets at a ratio of $80\%/10\%/10\%$. One positive label is randomly selected for each training instance, while the validation and test sets remain fully labeled. Detailed information regarding these datasets can be found in Appendix A.7. *Mean average precision (mAP)* is utilized for the four MLIC datasets [5, 33, 45] and five popular multi-label metrics are adopted for the MLL datasets including *Ranking loss, Hamming loss, One-error, Coverage* and *Average precision* [38].

[2]The detail is provided in Appendix A.4.

Table 2: Predictive performance of each comparing method on MLL datasets in terms of *Ranking loss* (mean ± std). The best performance is highlighted in bold (the smaller the better).

	Image	Scene	Yeast	Corel5k	Mirflickr	Delicious
AN	0.432±0.067	0.321±0.113	0.383±0.066	0.140±0.000	0.125±0.002	0.131±0.000
AN-LS	0.378±0.041	0.246±0.064	0.365±0.031	0.186±0.003	0.163±0.006	0.213±0.007
WAN	0.354±0.051	0.216±0.023	0.212±0.021	0.129±0.000	0.121±0.002	0.126±0.000
EPR	0.401±0.053	0.291±0.056	0.208±0.010	0.139±0.000	0.119±0.001	0.126±0.000
ROLE	0.340±0.059	0.174±0.028	0.213±0.017	0.259±0.004	0.182±0.014	0.336±0.007
EM	0.471±0.044	0.322±0.115	0.261±0.030	0.155±0.002	0.134±0.004	0.164±0.001
EM-APL	0.508±0.028	0.420±0.069	0.245±0.026	0.135±0.001	0.138±0.003	0.163±0.003
SMILE	0.260±0.020	0.161±0.045	0.167±0.002	0.125±0.003	0.120±0.002	0.126±0.000
LL-R	0.346±0.072	0.155±0.021	0.227±0.001	0.114±0.001	0.123±0.003	0.129±0.002
LL-CP	0.329±0.041	0.148±0.017	0.215±0.000	0.114±0.003	0.124±0.003	0.160±0.001
LL-CT	0.327±0.019	0.180±0.038	0.238±0.001	0.115±0.001	0.124±0.002	0.160±0.000
CRISP	**0.164±0.027**	**0.112±0.021**	**0.164±0.001**	**0.113±0.001**	**0.118±0.001**	**0.122±0.000**

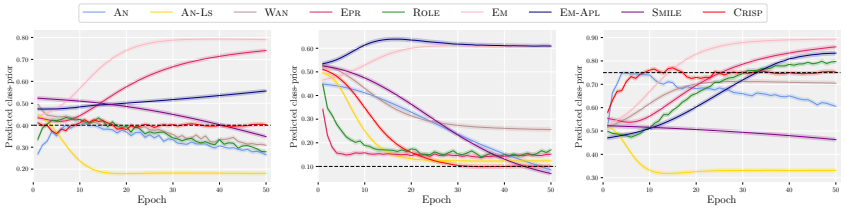

Figure 1: Predicted class-prior of AN[5], AN-LS[5], WAN[5], EPR[5], ROLE[5], EM[5], EM-APL[45], SMILE[38] and CRISP on the 3-*rd* (left), 10-*th* (middle), and 12-*th* labels (right) of the dataset `Yeast`.

Comparing methods. In this paper, CRISP is compared against nine state-of-the-art SPMLL approaches including: 1) AN [5] assumes that the unannotated labels are negative and uses binary cross entropy loss for training. 2) AN-LS [5] assumes that the unannotated labels are negative and reduces the impact of the false negative labels by label smoothing. 3) WAN [5] introduces a weight parameter to down-weight losses in relation to negative labels. 4) EPR [5] utilizes a regularization to constrain the number of predicted positive labels. 5) ROLE [5] online estimates the unannotated labels as learnable parameters throughout training based on EPR with the trick of linear initial. 6) EM [45] reduces the effect of the incorrect labels by the entropy-maximization loss. 7) EM-APL [45] adopts asymmetric-tolerance pseudo-label strategies cooperating with entropy-maximization loss and then more precise supervision can be provided. 8) PLC [33] designs a label-aware global consistency regularization to recover the pseudo-labels leveraging the manifold structure information learned by contrastive learning with data augmentation techniques. 9) SMILE [38] recovers the latent soft labels in a label enhancement process to train the multi-label classifier with binary cross entropy loss. Additionally, since the SPMLL problem is an extreme case of the MLML problem, we employ a state-of-the-art MLML methods as comparative methods: 1) LL [12] treats unobserved labels as noisy labels and dynamically adjusts the threshold to reject or correct samples with a large loss, including three variants LL-R, LL-CT and LL-CP. 2) BOOSTLU [13] apply a BoostLU function to the CAM output of the model to boost the scores of the highlighted regions. It can be integrated with LL. The implementation details are provided in Appendix A.6.

5.2 Experimental Results

Table 1 presents the comparison results of CRISP compared with other methods on `VOC`, `COCO`, `NUS`, and `CUB`. The proposed method achieves the best performance on `VOC`, `COCO`, and `NUS`. Although it does not surpass the top-performing method on `CUB`, the performance remains competitive. Table 2 record the results of our method and other comparing methods on the MLL datasets in terms of *Ranking loss* respectively. Similar results for other metrics can be found in Appendix A.8. Note that due to the inability to compute the loss function of PLC without data augmentation, we do not report the results of PLC on MLL datasets because data augmentation techniques are not suitable for the MLL datasets. Similarly, since the operations of BOOSTLU for CAM are not applicable to the tabular data in MLL datasets, its results are also not reported. The results demonstrate that our proposed method consistently achieves desirable performance in almost all cases (except the result of `Mirflickr` on the metric *Average Precision*, where our method attains a comparable performance

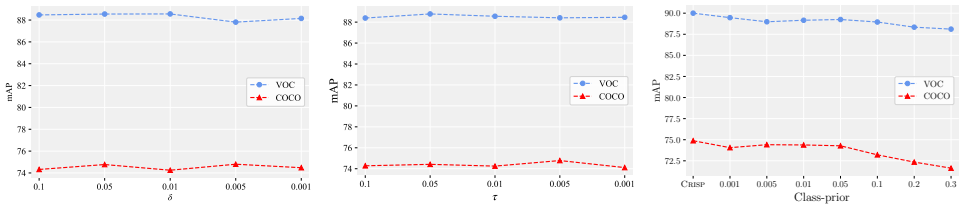

(a) Sensitivity analysis of δ (b) Sensitivity analysis of τ (c) Ablation results

Figure 2: (a) Parameter sensitivity analysis of δ (parameter τ is fixed as 0.01); (b) Parameter sensitivity analysis of τ (parameter δ is fixed as 0.01); (c) The initial data point represents the performance of the proposed CRISP (with class-priors estimator). The others are the performance with a fixed value for all class-priors gradually increasing from 0.001 to 0.3.

against SMILE). Table 12 in Appendix A.10 reports the p-values of the wilcoxon signed-ranks test [6] for the corresponding tests and the statistical test results at 0.05 significance level, which reveals that CRISP consistently outperforms other comparing algorithms (49 out of 55 test cases score **win**). These experimental results validate the effectiveness of CRISP in addressing SPMLL problems.

5.3 Further Analysis

5.3.1 Class-Prior Prediction

Figure 1 illustrates the comparison results of the predicted class-priors of CRISP with other methods on the 3-*rd* (left), 10-*th* (middle), and 12-*th* labels (right) of the dataset `Yeast`. Compared with other approaches, whose predicted class-priors $p(\hat{y}_j = 1)$, which represents the expected value of the predicted, significantly deviate from the true class-priors, CRISP achieves consistent predicted class-priors with the ground-truth class-priors (black dashed lines). Without the constraint of the class-priors, the predicted class-prior probability diverges from the true class-prior as epochs increase, significantly impacting the model's performance. In this experiment, the true class-priors are derived by calculating the statistical information for each dataset. More experimental results about the convergence analyses of estimated class-priors of all classes on MLIC datasets are recorded in Appendix A.9. These results demonstrate the necessity of incorporating class-priors in the training of the SPMLL model.

5.3.2 Sensitivity Analysis

The performance sensitivity of the proposed CRISP approach with respect to its parameters δ and τ during the class-priors estimation phase is analyzed in this section. Figures 2a and 2b illustrate the performance of the proposed method on `VOC` and `COCO` under various parameter settings, where δ and τ are incremented from 0.001 to 0.1. The performance of the proposed method remains consistently stable across a wide range of parameter values. This characteristic is highly desirable as it allows for the robust application of the proposed method without the need for meticulous parameter fine-tuning, ensuring reliable classification results.

5.3.3 Ablation Study

Figure 2c depicts the results of the ablation study to investigate the impact of the class-priors estimator by comparing it with a fixed value for all class-priors. The initial data point represents the performance of the proposed CRISP (with class-priors estimator). Subsequently, we maintain a fixed identical class-priors, gradually increasing it from 0.001 to 0.3. As expected, our method exhibits superior performance when utilizing the class-priors estimator, compared with employing a fixed class-prior proportion. The ablation results demonstrate the significant enhancement in CRISP performance achieved through the proposed class-priors estimator.

Table 3: Predictive performance comparing CRISP with CRISP-VAL.

Dataset	CRISP-VAL	CRISP
VOC	89.585±0.318	**89.820±0.191**
COCO	74.435±0.148	**74.640±0.219**
NUS	49.230±0.113	**49.996±0.316**
CUB	19.600±1.400	**21.650±0.178**

Table 4: Time cost of class-priors estimation and the whole training time of one epoch.

	VOC	COCO	NUS	CUB
Time of class-priors estimation (min)	0.24	3.47	6.4	0.45
Whole training time of one epoch (min)	2.19	27.29	49.09	3.89

Table 5: Predictive performance with different updating frequency of class-priors estimation.

	VOC	COCO	NUS	CUB
CRISP-3EP	89.077±0.251	73.930±0.399	49.463±0.216	19.450±0.389
CRISP	89.820±0.191	74.640±0.219	49.996±0.316	21.650±0.178

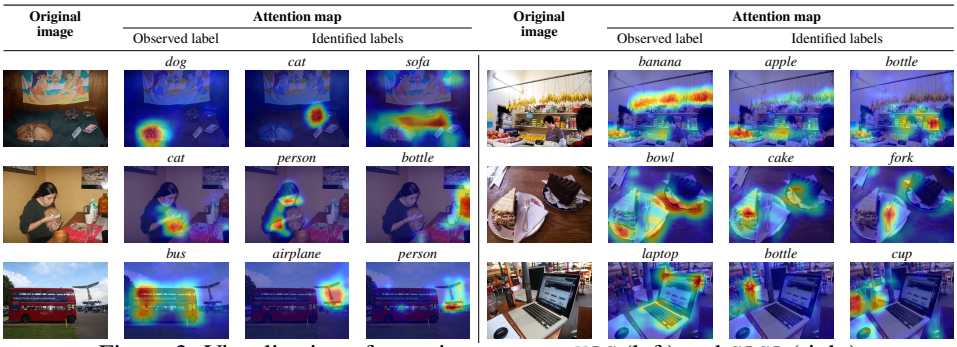

Figure 3: Visualization of attention maps on VOC (left) and COCO (right).

Furthermore, we conduct experiments comparing the performance of CRISP with the approach that estimating the class-priors with the full labels of validation set (CRISP-VAL). Table 3 shows that the performance of CRISP is superior to CRISP-VAL. It is indeed feasible to estimate the class-priors using the validation set. However, the size of validation set in many datasets is often quite small, which can lead to unstable estimation of the class-priors, thus leading to a suboptimal performance. Similar results are observed in Table 13 of Appendix A.11 for the MLL datasets.

5.3.4 Time Cost of Class-Priors Estimation

In Eq. (2), we have adopted an exhaustive search strategy to find an optimal threshold for estimating class-priors in each training epoch, which may introduce additional computational overhead to the algorithm. We conducted experimental analysis on this aspect. As illustrated in the Table 4, the time for class-priors estimation is short compared to the overall training time for an epoch, ensuring that our method remains practical for use in larger datasets. Additionally, to further enhance the speed of our algorithm, we have experimented with updating the class-priors every few epochs instead of every single one in Table 5. The variant of our method, denoted as CRISP-3EP, updates the priors every three epochs and our experiments show that this results in a negligible loss in performance.

5.3.5 Attention Map Visualization

Figure 3 is utilized to visually represent attention maps on COCO, elucidating the underlying mechanism responsible for the efficacy of CRISP in discerning potential positive labels. Specifically, for each original image in the first column, attention maps corresponding to the single observed positive label and identified positive labels are displayed in the subsequent three columns. As evidenced by the figures, given the context of a single positive label, the proposed method demonstrates the ability to identify additional object labels within the image, even for relatively small objects such as the bottle in the first row, the fork in the second row, and the cup in the final row. These observations indicate that the proposed method can accurately detect small objects with the aid of class-priors. This insight further suggests that the proposed method substantially enhances the model's capacity to pinpoint potential positive labels.

6 Conclusion

In conclusion, this paper presents a novel approach to address the single-positive multi-label learning (SPMLL) problem by considering the impact of class-priors on the model. We propose a theoretically guaranteed class-priors estimation method that ensures the convergence of estimated class-prior to ground-truth class-priors during the training process. Furthermore, we introduce an unbiased risk estimator based on the estimated class-priors and derive a generalization error bound to guarantee

that the obtained risk minimizer would approximately converge to the optimal risk minimizer of fully supervised learning. Experimental results on ten MLL benchmark datasets demonstrate the effectiveness and superiority of our method over existing SPMLL approaches.

7 Acknowledgments

This research was supported by the Jiangsu Science Foundation (BG2024036, BK20243012), the National Science Foundation of China (62576093, 62206050, 62125602, U24A20324, and 92464301), the Fundamental Research Funds for the Central Universities (2242025K30024), and the Big Data Computing Center of Southeast University.

References

[1] Matthew R Boutell, Jiebo Luo, Xipeng Shen, and Christopher M Brown. Learning multi-label scene classification. *Pattern recognition*, 37(9):1757–1771, 2004.

[2] Shikai Chen, Jianfeng Wang, Yuedong Chen, Zhongchao Shi, Xin Geng, and Yong Rui. Label distribution learning on auxiliary label space graphs for facial expression recognition. In *Proceedings of the IEEE/CVF Conference on Computer Vision and Pattern Recognition*, pages 13981–13990, Seattle, WA, 2020.

[3] Zhao-Min Chen, Xiu-Shen Wei, Peng Wang, and Yanwen Guo. Multi-label image recognition with graph convolutional networks. In *Proceedings of the IEEE/CVF Conference on Computer Vision and Pattern Recognition*, pages 5177–5186, Long Beach, CA, 2019.

[4] Tat-Seng Chua, Jinhui Tang, Richang Hong, Haojie Li, Zhiping Luo, and Yantao Zheng. NUS-WIDE: a real-world web image database from national university of singapore. In *Proceedings of the 8th ACM International Conference on Image and Video Retrieval*, Santorini Island, Greece, 2009.

[5] Elijah Cole, Oisin Mac Aodha, Titouan Lorieul, Pietro Perona, Dan Morris, and Nebojsa Jojic. Multi-label learning from single positive labels. In *Proceedings of the IEEE/CVF Conference on Computer Vision and Pattern Recognition*, pages 933–942, virtual, 2021.

[6] Janez Demšar. Statistical comparisons of classifiers over multiple data sets. *The Journal of Machine learning research*, 7:1–30, 2006.

[7] André Elisseeff and Jason Weston. A kernel method for multi-labelled classification. In *Advances in Neural Information Processing Systems 14*, pages 681–687, Vancouver, BC, Canada, 2001.

[8] Mark Everingham, Luc Van Gool, Christopher K. I. Williams, John M. Winn, and Andrew Zisserman. The pascal visual object classes (VOC) challenge. *International Journal of Computer Vision*, 88(2):303–338, 2010.

[9] Johannes Fürnkranz, Eyke Hüllermeier, Eneldo Loza Mencía, and Klaus Brinker. Multilabel classification via calibrated label ranking. *Machine learning*, 73(2):133–153, 2008.

[10] Saurabh Garg, Yifan Wu, Alexander J. Smola, Sivaraman Balakrishnan, and Zachary C. Lipton. Mixture proportion estimation and PU learning: A modern approach. In *Advances in Neural Information Processing Systems 34*, pages 8532–8544, Virtual, 2021.

[11] Jun-Yi Hang and Min-Ling Zhang. Collaborative learning of label semantics and deep label-specific features for multi-label classification. *IEEE Transactions on Pattern Analysis and Machine Intelligence*, 44(12):9860–9871, 2022.

[12] Youngwook Kim, Jae Myung Kim, Zeynep Akata, and Jungwoo Lee. Large loss matters in weakly supervised multi-label classification. In *Proceedings of the IEEE/CVF Conference on Computer Vision and Pattern Recognition*, pages 14156–14165, New Orleans, LA, 2022.

[13] Youngwook Kim, Jae-Myung Kim, Jieun Jeong, Cordelia Schmid, Zeynep Akata, and Jungwoo Lee. Bridging the gap between model explanations in partially annotated multi-label classification. In *Proceedings of the IEEE/CVF Conference on Computer Vision and Pattern Recognition*, pages 3408–3417, Vancover, BC, Canada, 2023.

[14] Zhiqiang Kou, Si Qin, Hailin Wang, Jing Wang, Mingkun Xie, Shuo Chen, Yuheng Jia, Tongliang Liu, Masashi Sugiyama, and Xin Geng. Label distribution learning with biased annotations assisted by multi-label learning. In *Proceedings of International Joint Conference on Artificial Intelligence*, Montreal, Canada, 2025.

[15] Zhiqiang Kou, Jing Wang, Yuheng Jia, and Xin Geng. Inaccurate label distribution learning. *IEEE Transactions on Circuits and Systems for Video Technology*, 34(10):10237–10249, 2024.

[16] Zhiqiang Kou, Jing Wang, Yuheng Jia, and Xin Geng. Progressive label enhancement. *Pattern Recognition*, 160:111172, 2025.

[17] Zhiqiang Kou, Jing Wang, Yuheng Jia, Biao Liu, and Xin Geng. Instance-dependent inaccurate label distribution learning. *IEEE Transactions on Neural Networks and Learning Systems*, 36(1):1425–1437, 2025.

[18] Zhiqiang Kou, Jing Wang, Jiawei Tang, Yuheng Jia, Boyu Shi, and Xin Geng. Exploiting multi-label correlation in label distribution learning. In *Proceedings of International Joint Conference on Artificial Intelligence*, pages 4326–4334, Jeju Island, Korea, 2024.

[19] Zhiqiang Kou, Haoyuan Xuan, Jingyu Zhu, Hailin Wang, Ming-kun Xie, Changwei Wang, Jing Wang, Yuheng Jia, and Xin Geng. Tail-aware reconstruction of incomplete label distributions with low-rank and sparse modeling. *IEEE Transactions on Circuits and Systems for Video Technology*, 2025.

[20] Tsung-Yi Lin, Michael Maire, Serge J. Belongie, James Hays, Pietro Perona, Deva Ramanan, Piotr Dollár, and C. Lawrence Zitnick. Microsoft COCO: common objects in context. In *Proceedings of 13th European Conference on Computer Vision*, volume 8693, pages 740–755, Zurich, Switzerland, 2014.

[21] Biao Liu, Ning Xu, Xiangyu Fang, and Xin Geng. Correlation-induced label prior for semi-supervised multi-label learning. In *Proceedings of the 41st International Conference on Machine Learning*, volume 235, pages 32224–32238, Vienna, Austria, 2024.

[22] Biao Liu, Ning Xu, and Xin Geng. Progressively label enhancement for large language model alignment. In *Proceedings of the 42nd International Conference on Machine Learning*, volume 267, pages 39915–39928, Vancouver, Canada, 2025.

[23] Biao Liu, Ning Xu, Jiaqi Lv, and Xin Geng. Revisiting pseudo-label for single-positive multi-label learning. In *Proceedings of International Conference on Machine Learning*, volume 202, pages 22249–22265, Honolulu, Hawaii, 2023.

[24] Jingzhou Liu, Wei-Cheng Chang, Yuexin Wu, and Yiming Yang. Deep learning for extreme multi-label text classification. In *Proceedings of the 40-th International ACM SIGIR Conference on Research and Development in Information Retrieval*, pages 115–124, Tokyo, Japan, 2017.

[25] Weiwei Liu, Haobo Wang, Xiaobo Shen, and Ivor W Tsang. The emerging trends of multi-label learning. *IEEE Transactions on Pattern Analysis and Machine Intelligence*, 44(11):7955–7974, 2021.

[26] Mehryar Mohri, Afshin Rostamizadeh, and Ameet Talwalkar. *Foundations of Machine Learning*. Adaptive computation and machine learning. MIT Press, 2012.

[27] Jesse Read, Bernhard Pfahringer, Geoff Holmes, and Eibe Frank. Classifier chains for multi-label classification. *Machine learning*, 85(3):333–359, 2011.

[28] Yu-Yin Sun, Yin Zhang, and Zhi-Hua Zhou. Multi-label learning with weak label. In *Proceedings of the 24th AAAI Conference on Artificial Intelligence*, Atlanta, Georgia, 2010.

[29] Catherine Wah, Steve Branson, Peter Welinder, Pietro Perona, and Serge Belongie. The caltech-ucsd birds-200-2011 dataset. California Institute of Technology, 2011.

[30] Changhu Wang, Shuicheng Yan, Lei Zhang, and Hong-Jiang Zhang. Multi-label sparse coding for automatic image annotation. In *Proceedings of the IEEE/CVF Conference on Computer Vision and Pattern Recognition*, pages 1643–1650, Miami, Florida, 2009.

[31] Kaixiang Wang. Robust embedding framework with dynamic hypergraph fusion for multi-label classification. In *Proceedings of the IEEE International Conference on Multimedia and Expo*, pages 982–987, Shanghai, China, 2019.

[32] Baoyuan Wu, Zhilei Liu, Shangfei Wang, Bao-Gang Hu, and Qiang Ji. Multi-label learning with missing labels. In *Proceedings of the 22nd International Conference on Pattern Recognition*, pages 1964–1968, Stockholm, Sweden, 2014.

[33] Ming-Kun Xie, Jia-Hao Xiao, and Sheng-Jun Huang. Label-aware global consistency for multi-label learning with single positive labels. In *Advances in Neural Information Processing Systems*, virtual, 2022.

[34] Chang Xu, Dacheng Tao, and Chao Xu. Robust extreme multi-label learning. In *Proceedings of the 22nd ACM SIGKDD International Conference on Knowledge Discovery and Data Mining*, pages 1275–1284, San Francisco, CA, 2016.

[35] Miao Xu, Rong Jin, and Zhi-Hua Zhou. Speedup matrix completion with side information: Application to multi-label learning. In *Advances in Neural Information Processing Systems 26*, pages 2301–2309, Lake Tahoe, Nevada, 2013.

[36] Ning Xu, Biao Liu, Jiaqi Lv, Congyu Qiao, and Xin Geng. Progressive purification for instance-dependent partial label learning. In *Proceedings of the 40th International Conference on Machine Learning*, volume 202, pages 38551–38565, Honolulu, Hawaii, 2023.

[37] Ning Xu, Yun-Peng Liu, and Xin Geng. Label enhancement for label distribution learning. *IEEE Transactions on Knowledge and Data Engineering*, 33(4):1632–1643, 2021.

[38] Ning Xu, Congyu Qiao, Jiaqi Lv, Xin Geng, and Min-Ling Zhang. One positive label is sufficient: Single-positive multi-label learning with label enhancement. In *Advances in Neural Information Processing Systems*, virtual, 2022.

[39] Chih-Kuan Yeh, Wei-Chieh Wu, Wei-Jen Ko, and Yu-Chiang Frank Wang. Learning deep latent space for multi-label classification. In *Proceedings of the 21st AAAI Conference on Artificial Intelligence*, pages 2838–2844, San Francisco, California, 2017.

[40] Hsiang-Fu Yu, Prateek Jain, Purushottam Kar, and Inderjit S. Dhillon. Large-scale multi-label learning with missing labels. In *Proceedings of the 31th International Conference on Machine Learning*, volume 32, pages 593–601, Beijing, China, 2014.

[41] Ze-Bang Yu and Min-Ling Zhang. Multi-label classification with label-specific feature generation: A wrapped approach. *IEEE Transactions on Pattern Analysis and Machine Intelligence*, 44(9):5199–5210, 2022.

[42] Sangdoo Yun, Seong Joon Oh, Byeongho Heo, Dongyoon Han, Junsuk Choe, and Sanghyuk Chun. Re-labeling imagenet: From single to multi-labels, from global to localized labels. In *Proceedings of the IEEE/CVF Conference on Computer Vision and Pattern Recognition*, pages 2340–2350, virtual, 2021.

[43] Min-Ling Zhang and Zhi-Hua Zhou. A review on multi-label learning algorithms. *IEEE Transactions on Knowledge and Data Engineering*, 26(8):1819–1837, 2013.

[44] Yunrui Zhao, Qianqian Xu, Yangbangyan Jiang, Peisong Wen, and Qingming Huang. Dist-pu: Positive-unlabeled learning from a label distribution perspective. In *Proceedings of the IEEE/CVF Conference on Computer Vision and Pattern Recognition*, pages 14461–14470, New Orleans, LA, 2022.

[45] Donghao Zhou, Pengfei Chen, Qiong Wang, Guangyong Chen, and Pheng-Ann Heng. Acknowledging the unknown for multi-label learning with single positive labels. In *Proceedings of 17th European Conference on Computer Vision*, volume 13684, pages 423–440, Tel Aviv, Israel, 2022.

A Supplementary Material

A.1 Proof of Theorem 4.1

Proof. Firstly, we have:

$$\begin{aligned}\Big|\frac{\hat{q}_j(z)}{\hat{q}_j^p(z)} - \frac{q_j(z)}{q_j^p(z)}\Big| &= \frac{\hat{q}_j(z)q_j^p(z) - \hat{q}_j^p(z)q_j(z)}{\hat{q}_j^p(z)q_j^p(z)} \\ &\leq \frac{|\hat{q}_j(z)q_j^p(z) - q_j^p(z)q_j(z)| + |q_j^p(z)q_j(z) - \hat{q}_j^p(z)q_j(z)|}{\hat{q}_j^p(z)q_j^p(z)} \\ &= \frac{1}{\hat{q}_j^p(z)}|\hat{q}_j(z) - q_j(z)| + \frac{q_j(z)}{\hat{q}_j^p(z)q_j^p(z)}|\hat{q}_j^p(z) - q_j^p(z)|,\end{aligned} \tag{9}$$

where z is an arbitrary constant in $[0,1]$. Using DKW inequality, we have with probability $1-\delta$: $|\hat{q}_j(z) - q_j(z)| \leq \sqrt{\frac{\log 2/\delta}{2n}}$ and $|\hat{q}_j^p(z) - q_j^p(z)| \leq \sqrt{\frac{\log 2/\delta}{2n_j^p}}$. Therefore, with probability $1-\delta$:

$$\Big|\frac{\hat{q}_j(z)}{\hat{q}_j^p(z)} - \frac{q_j(z)}{q_j^p(z)}\Big| \leq \frac{1}{\hat{q}_j^p(z)}\left(\sqrt{\frac{\log 4/\delta}{2n}} + \frac{q_j(z)}{q_j^p(z)}\sqrt{\frac{\log 4/\delta}{2n_j^p}}\right). \tag{10}$$

Then, we define:

$$\begin{aligned}\hat{z} &= \arg\min_{z\in[0,1]}\left(\frac{\hat{q}_j(z)}{\hat{q}_j^p(z)} + \frac{1+\tau}{\hat{q}_j^p(z)}\left(\sqrt{\frac{\log(4/\delta)}{2n}} + \sqrt{\frac{\log(4/\delta)}{2n_j^p}}\right)\right), \\ z^\star &= \arg\min_{z\in[0,1]}\frac{q_j(z)}{q_j^p(z)}, \\ \hat{\pi}_j &= \frac{\hat{q}_j(\hat{z})}{\hat{q}_j^p(\hat{z})} \qquad \text{and} \qquad \pi_j^\star = \frac{q_j(z^\star)}{q_j^p(z^\star)}.\end{aligned}$$

Next, consider $z' \in [0,1]$ such that $\hat{q}_j^p(z') = \frac{\tau}{2+\tau}\hat{q}_j^p(z^\star)$. We now show that $\hat{z} < z'$. For any $z \in [0,1]$, by the DWK inequality, we have with probability $1-\delta$:

$$\begin{aligned}\hat{q}_j^p(z) - \sqrt{\frac{\log 4/\delta}{2n_j^p}} &\leq q_j^p(z), \\ q_j(z) - \sqrt{\frac{\log 4/\delta}{2n}} &\leq \hat{q}_j(z).\end{aligned} \tag{11}$$

Since $\frac{q_j(z^\star)}{q_j^p(z^\star)} \leq \frac{q_j(z)}{q_j^p(z)}$, we have:

$$\hat{q}_j(z) \geqslant q_j^p(z)\frac{q_j\left(z^\star\right)}{q_j^p\left(z^\star\right)} - \sqrt{\frac{\log(4/\delta)}{2n}} \geqslant \left(\hat{q}_j^p(z) - \sqrt{\frac{\log(4/\delta)}{2n_j^p}}\right)\frac{q_j\left(z^\star\right)}{q_j^p\left(z^\star\right)} - \sqrt{\frac{\log(4/\delta)}{2n}}. \tag{12}$$

Therefore, we have:

$$\frac{\hat{q}_j(z)}{\hat{q}_j^p(z)} \geq \pi_j^\star - \frac{1}{\hat{q}_j^p(z)}\left(\sqrt{\frac{\log(4/\delta)}{2n}} + \pi_j^\star\sqrt{\frac{\log(4/\delta)}{2n_j^p}}\right). \tag{13}$$

Using Eq. (10) at $z^\star$ and the fact that $\pi_j^\star = \frac{q_j(z^\star)}{q_j^p(z^\star)} \leq 1$, we have:

$$\begin{aligned}\frac{\hat{q}_j(z)}{\hat{q}_j^p(z)} &\geq \frac{\hat{q}_j(z^\star)}{\hat{q}_j^p(z^\star)} - \left(\frac{1}{\hat{q}_j^p(z^\star)} + \frac{1}{\hat{q}_j^p(z)}\right)\left(\sqrt{\frac{\log(4/\delta)}{2n}} + \pi_j^\star\sqrt{\frac{\log(4/\delta)}{2n_j^p}}\right) \\ &\geq \frac{\hat{q}_j(z^\star)}{\hat{q}_j^p(z^\star)} - \left(\frac{1}{\hat{q}_j^p(z^\star)} + \frac{1}{\hat{q}_j^p(z)}\right)\left(\sqrt{\frac{\log(4/\delta)}{2n}} + \sqrt{\frac{\log(4/\delta)}{2n_j^p}}\right).\end{aligned} \tag{14}$$

Furthermore, the upper confidence bound at z is lower bounded by:

$$\begin{aligned}
&\frac{\hat{q}_j(z)}{\hat{q}_j^p(z)} + \frac{1+\tau}{\hat{q}_j^p(z)}\left(\sqrt{\frac{\log(4/\delta)}{2n}} + \sqrt{\frac{\log(4/\delta)}{2n_j^p}}\right) \\
&\geq \frac{\hat{q}_j(z^\star)}{\hat{q}_j^p(z^\star)} + \left(\frac{1+\tau}{\hat{q}_j^p(z)} - \frac{1}{\hat{q}_j^p(z^\star)} - \frac{1}{\hat{q}_j^p(z)}\right)\left(\sqrt{\frac{\log(4/\delta)}{2n}} + \sqrt{\frac{\log(4/\delta)}{2n_j^p}}\right) \\
&= \frac{\hat{q}_j(z^\star)}{\hat{q}_j^p(z^\star)} + \left(\frac{\tau}{\hat{q}_j^p(z)} - \frac{1}{\hat{q}_j^p(z^\star)}\right)\left(\sqrt{\frac{\log(4/\delta)}{2n}} + \sqrt{\frac{\log(4/\delta)}{2n_j^p}}\right).
\end{aligned} \tag{15}$$

Using Eq. (15) at $z = z'$ where $\hat{q}_j^p(z') = \frac{\tau}{2+\tau}\hat{q}_j^p(z^\star)$, we have:

$$\begin{aligned}
&\frac{\hat{q}_j(z')}{\hat{q}_j^p(z')} + \frac{1+\tau}{\hat{q}_j^p(z')}\left(\sqrt{\frac{\log(4/\delta)}{2n}} + \sqrt{\frac{\log(4/\delta)}{2n_j^p}}\right) \\
&\geq \frac{\hat{q}_j(z^\star)}{\hat{q}_j^p(z^\star)} + \left(\frac{\tau}{\hat{q}_j^p(z')} - \frac{1}{\hat{q}_j^p(z^\star)}\right)\left(\sqrt{\frac{\log(4/\delta)}{2n}} + \sqrt{\frac{\log(4/\delta)}{2n_j^p}}\right). \\
&\geq \frac{\hat{q}_j(z^\star)}{\hat{q}_j^p(z^\star)} + \frac{1+\tau}{\hat{q}_j^p(z^\star)}\left(\sqrt{\frac{\log(4/\delta)}{2n}} + \sqrt{\frac{\log(4/\delta)}{2n_j^p}}\right).
\end{aligned} \tag{16}$$

Moreover from Eq. (15) and using definition of $\hat{z}$, we have:

$$\begin{aligned}
&\frac{\hat{q}_j(z')}{\hat{q}_j^p(z')} + \frac{1+\tau}{\hat{q}_j^p(z')}\left(\sqrt{\frac{\log(4/\delta)}{2n}} + \sqrt{\frac{\log(4/\delta)}{2n_j^p}}\right) \\
&\geq \frac{\hat{q}_j(z^\star)}{\hat{q}_j^p(z^\star)} + \frac{1+\tau}{\hat{q}_j^p(z^\star)}\left(\sqrt{\frac{\log(4/\delta)}{2n}} + \sqrt{\frac{\log(4/\delta)}{2n_j^p}}\right) \\
&\geq \frac{\hat{q}_j(\hat{z})}{\hat{q}_j^p(\hat{z})} + \frac{1+\tau}{\hat{q}_j^p(\hat{z})}\left(\sqrt{\frac{\log(4/\delta)}{2n}} + \sqrt{\frac{\log(4/\delta)}{2n_j^p}}\right),
\end{aligned} \tag{17}$$

and hence $\hat{z} \leq z'$.

We now establish an upper and lower bound on $\hat{z}$. By definition of $\hat{z}$, we have:

$$\begin{aligned}
&\frac{\hat{q}_j(\hat{z})}{\hat{q}_j^p(\hat{z})} + \frac{1+\tau}{\hat{q}_j^p(\hat{z})}\left(\sqrt{\frac{\log(4/\delta)}{2n}} + \sqrt{\frac{\log(4/\delta)}{2n_j^p}}\right) \\
&\leq \min_{z\in[0,1]}\left(\frac{\hat{q}_j(z)}{\hat{q}_j^p(z)} + \frac{1+\tau}{\hat{q}_j^p(z)}\left(\sqrt{\frac{\log(4/\delta)}{2n}} + \sqrt{\frac{\log(4/\delta)}{2n_j^p}}\right)\right) \\
&\leq \frac{\hat{q}_j(z^\star)}{\hat{q}_j^p(z^\star)} + \frac{1+\tau}{\hat{q}_j^p(z^\star)}\left(\sqrt{\frac{\log(4/\delta)}{2n}} + \sqrt{\frac{\log(4/\delta)}{2n_j^p}}\right).
\end{aligned} \tag{18}$$

Using Eq. (10) at $z^\star$, we have:

$$\frac{\hat{q}_j(z^\star)}{\hat{q}_j^p(z^\star)} \leq \frac{q_j(z^\star)}{q_j^p(z^\star)} + \frac{1}{\hat{q}_j^p(z^\star)}\left(\sqrt{\frac{\log(4/\delta)}{2n}} + \pi_j^\star\sqrt{\frac{\log(4/\delta)}{2n_j^p}}\right). \tag{19}$$

Then, we have:

$$\hat{\pi}_j = \frac{\hat{q}_j(\hat{z})}{\hat{q}_j^p(\hat{z})} \leq \pi_j^\star + \frac{2+\tau}{\hat{q}_j^p(z^\star)}\left(\sqrt{\frac{\log(4/\delta)}{2n}} + \sqrt{\frac{\log(4/\delta)}{2n_j^p}}\right). \tag{20}$$

Assume $n_j^p \geq 2\frac{\log 4/\delta}{{q_j^p}^2(z^\star)}$, we have $\hat{q}_j^p(z^\star) \geq q_j^p(z^\star)/2$ and hence:

$$\hat{\pi}_j \leq \pi_j^\star + \frac{4+2\tau}{q_j^p(z^\star)}\left(\sqrt{\frac{\log(4/\delta)}{2n}} + \sqrt{\frac{\log(4/\delta)}{2n_j^p}}\right). \tag{21}$$

From Eq. (10) at $\hat{z}$, we have:

$$\frac{q_j(\hat{z})}{q_j^p(\hat{z})} \leq \frac{\hat{q}_j(\hat{z})}{\hat{q}_j^p(\hat{z})} + \frac{1}{\hat{q}_j^p(\hat{z})}\left(\sqrt{\frac{\log(4/\delta)}{2n}} + \frac{q_j(\hat{z})}{q_j^p(\hat{z})}\sqrt{\frac{\log(4/\delta)}{2n_j^p}}\right). \tag{22}$$

Since $\pi_j^\star \leq \frac{q_j(\hat{z})}{q_j^p(\hat{z})}$, we have:

$$\pi_j^\star \leq \frac{q_j(\hat{z})}{q_j^p(\hat{z})} \leq \frac{\hat{q}_j(\hat{z})}{\hat{q}_j^p(\hat{z})} + \frac{1}{\hat{q}_j^p(\hat{z})}\left(\sqrt{\frac{\log(4/\delta)}{2n}} + \frac{q_j(\hat{z})}{q_j^p(\hat{z})}\sqrt{\frac{\log(4/\delta)}{2n_j^p}}\right). \tag{23}$$

Using Eq. (21) and the assumption that $n \geq n_j^p \geq 2\frac{\log 4/\delta}{{q_j^p}^2(z^\star)}$, we have:

$$\begin{aligned}\hat{\pi}_j = \frac{\hat{q}_j(\hat{z})}{\hat{q}_j^p(\hat{z})} &\leq \pi_j^\star + \frac{4+2\tau}{q_j^p(z^\star)}\left(\sqrt{\frac{\log(4/\delta)}{2n}} + \sqrt{\frac{\log(4/\delta)}{2n_j^p}}\right) \\ &\leq \pi_j^\star + 4 + 2\tau \leq 1 + 4 + 2\tau = 5 + 2\tau.\end{aligned} \tag{24}$$

Using this in Eq. (23), we have:

$$\pi_j^\star \leq \frac{\hat{q}_j(\hat{z})}{\hat{q}_j^p(\hat{z})} + \frac{1}{\hat{q}_j^p(\hat{z})}\left(\sqrt{\frac{\log(4/\delta)}{2n}} + (5+2\tau)\sqrt{\frac{\log(4/\delta)}{2n_j^p}}\right). \tag{25}$$

Since $\hat{z} \leq z'$, we have $\hat{q}_j^p(\hat{z}) \geq \hat{q}_j^p(z') = \frac{\tau}{2+\tau}\hat{q}_j^p(z^\star)$. Therefore, we have:

$$\pi_j^\star - \frac{2+\tau}{\tau\hat{q}_j^p(z^\star)}\left(\sqrt{\frac{\log(4/\delta)}{2n}} + (5+2\tau)\sqrt{\frac{\log(4/\delta)}{2n_j^p}}\right) \leq \frac{\hat{q}_j(\hat{z})}{\hat{q}_j^p(\hat{z})} = \hat{\pi}_j. \tag{26}$$

With the assumption that $n_j^p \geq 2\frac{\log 4/\delta}{{q_j^p}^2(z^\star)}$, we have $\hat{q}_j^p(z^\star) \geq q_j^p(z^\star)/2$, which implies:

$$\pi_j^\star - \frac{4+2\tau}{\tau q_j^p(z^\star)}\left(\sqrt{\frac{\log(4/\delta)}{2n}} + (5+2\tau)\sqrt{\frac{\log(4/\delta)}{2n_j^p}}\right) \leq \hat{\pi}_j. \tag{27}$$

Note that since $\pi_j \leq \pi_j^\star$, the lower bound remains the same as in Theorem 4.1. For the upper bound, with $q_j(z^\star) = \pi_j q_j^p(z^\star) + (1-\pi_j)q_j^n(z^\star)$, we have $\pi_j^\star = \pi_j + (1-\pi_j)\frac{q_j^n(z^\star)}{q_j^p(z^\star)}$. Then the proof is completed.

□

A.2 The details of the optimization of Eq. (2)

In practice, to determine the optimal threshold, we conduct an exhaustive search across the set of outputs generated by the function f^j for each class. For instance, for a given class j, and a set of instances $\boldsymbol{x}_1, \boldsymbol{x}_2, \boldsymbol{x}_3$ in our dataset, we compute the corresponding outputs $z_1 = f^j(\boldsymbol{x}_1), z_2 = f^j(\boldsymbol{x}_2), z_3 = f^j(\boldsymbol{x}_3)$.

The optimal threshold $\hat{z}$ is then selected by identifying the value of $z \in \{z_1, z_2, z_3\}$ that minimizes the objective function specified in Equation (2):

$$\hat{z} = \arg\min_{z \in \{z_1, z_2, z_3\}}\left(\frac{\hat{q}_j(z)}{\hat{q}_j^p(z)} + \frac{1+\tau}{\hat{q}_j^p(z)}\left(\sqrt{\frac{\log(4/\delta)}{2n}} + \sqrt{\frac{\log(4/\delta)}{2n_j^p}}\right)\right)$$

This approach ensures that we find the optimal threshold that minimizes the given expression, as per Eq. (2), across all available output values from the function f^j.

A.3 Details of Eq. (3)

$$\begin{aligned}\mathcal{R}(f) &= \mathbb{E}_{(\boldsymbol{x},\boldsymbol{y})\sim p(\boldsymbol{x},\boldsymbol{y})}\left[\mathcal{L}(f(\boldsymbol{x}),\boldsymbol{y})\right] \\ &= \int_{\boldsymbol{x}}\sum_{\boldsymbol{y}}\mathcal{L}(f(\boldsymbol{x}),\boldsymbol{y})p(\boldsymbol{x}|\boldsymbol{y})p(\boldsymbol{y})d\boldsymbol{x} \\ &= \sum_{\boldsymbol{y}}p(\boldsymbol{y})\int_{\boldsymbol{x}}\mathcal{L}(f(\boldsymbol{x}),\boldsymbol{y})p(\boldsymbol{x}|\boldsymbol{y})d\boldsymbol{x} \\ &= \sum_{\boldsymbol{y}}p(\boldsymbol{y})\mathbb{E}_{\boldsymbol{x}\sim p(\boldsymbol{x}|\boldsymbol{y})}\left[\mathcal{L}(f(\boldsymbol{x}),\boldsymbol{y})\right].\end{aligned} \tag{28}$$

A.4 Details of Eq. (5)

The absolute loss function is $\ell(f^j(\boldsymbol{x}),y_j)=|f^j(\boldsymbol{x})-y_j|$, when $y_j=1$, $\ell(f^j(\boldsymbol{x}),1)=|1-f^j(\boldsymbol{x})|$, and when $y_j=0$, $\ell(f^j(\boldsymbol{x}),0)=f^j(\boldsymbol{x})$. Then:

$$\begin{aligned}\mathcal{R}(f) &= \sum_{\boldsymbol{y}}p(\boldsymbol{y})\mathbb{E}_{\boldsymbol{x}\sim p(\boldsymbol{x}|\boldsymbol{y})}\left[\sum_{j=1}^{c}y_j\ell(f^j(\boldsymbol{x}),1)+(1-y_j)\ell(f^j(\boldsymbol{x}),0)\right] \\ &= \sum_{j=1}^{c}p(y_j=1)\mathbb{E}_{\boldsymbol{x}\sim p(\boldsymbol{x}|y_j=1)}\left[\ell(f^j(\boldsymbol{x}),1)\right]+p(y_j=0)\mathbb{E}_{\boldsymbol{x}\sim p(\boldsymbol{x}|y_j=0)}\left[\ell(f^j(\boldsymbol{x}),0)\right] \\ &= \sum_{j=1}^{c}p(y_j=1)\mathbb{E}_{\boldsymbol{x}\sim p(\boldsymbol{x}|y_j=1)}\left[1-f^j(\boldsymbol{x})\right]+(1-p(y_j=1))\mathbb{E}_{\boldsymbol{x}\sim p(\boldsymbol{x}|y_j=0)}\left[f^j(\boldsymbol{x})\right] \\ &= \sum_{j=1}^{c}p(y_j=1)\mathbb{E}_{\boldsymbol{x}\sim p(\boldsymbol{x}|y_j=1)}\left[1-f^j(\boldsymbol{x})\right]+\mathbb{E}_{\boldsymbol{x}\sim p(\boldsymbol{x})}\left[f^j(\boldsymbol{x})\right] \\ &\quad -p(y_j=1)\mathbb{E}_{\boldsymbol{x}\sim p(\boldsymbol{x}|y_j=1)}\left[f^j(\boldsymbol{x})\right] \\ &= \sum_{j=1}^{c}p(y_j=1)\mathbb{E}_{\boldsymbol{x}\sim p(\boldsymbol{x}|y_j=1)}\left[1-f^j(\boldsymbol{x})\right]+\mathbb{E}_{\boldsymbol{x}\sim p(\boldsymbol{x})}\left[f^j(\boldsymbol{x})\right] \\ &\quad -p(y_j=1)\mathbb{E}_{\boldsymbol{x}\sim p(\boldsymbol{x}|y_j=1)}\left[f^j(\boldsymbol{x})-1+1\right] \\ &= \sum_{j=1}^{c}2p(y_j=1)\mathbb{E}_{\boldsymbol{x}\sim p(\boldsymbol{x}|y_j=1)}\left[1-f^j(\boldsymbol{x})\right]+\mathbb{E}_{\boldsymbol{x}\sim p(\boldsymbol{x})}\left[f^j(\boldsymbol{x})\right]-p(y_j=1).\end{aligned} \tag{29}$$

A.5 Proof of Theorem 4.2

In this subsection, an estimation error bound is established for Eq. (7) to demonstrate its learning consistency. Specifically, The derivation of the estimation error bound involves two main parts, each corresponding to one of the loss terms in Eq. (7). The empirical risk estimator according to Eq. (7) can be written as:

$$\begin{aligned}\widehat{\mathcal{R}}_{sp}(f) &= \sum_{j=1}^{c}\frac{2\pi_j}{|\mathcal{S}_{L_j}|}\sum_{\boldsymbol{x}\in\mathcal{S}_{L_j}}\left(1-f^j(\boldsymbol{x})\right)+\frac{1}{n}\sum_{\boldsymbol{x}\in\widehat{\mathcal{D}}}\left(f^j(\boldsymbol{x})-\pi_j\right) \\ &= \widehat{\mathcal{R}}_{sp}^{L}(f)+\widehat{\mathcal{R}}_{sp}^{U}(f),\end{aligned} \tag{30}$$

Firstly, we define the function spaces as:

$$\mathcal{G}_{sp}^{L}=\left\{(\boldsymbol{x},\boldsymbol{l})\mapsto\sum_{j=1}^{c}2\pi_j l_j\left(1-f^j(\boldsymbol{x})\right)|f\in\mathcal{F}\right\},\mathcal{G}_{sp}^{U}=\left\{(\boldsymbol{x},\boldsymbol{l})\mapsto\sum_{j=1}^{c}\left(f^j(\boldsymbol{x})-\pi_j\right)|f\in\mathcal{F}\right\},$$

and denote the expected Rademacher complexity [26] of the function spaces as:

$$\widetilde{\mathfrak{R}}_n\left(\mathcal{G}_{sp}^L\right) = \mathbb{E}_{\boldsymbol{x},\boldsymbol{l},\boldsymbol{\sigma}}\left[\sup_{g\in\mathcal{G}_{sp}^L}\sum_{i=1}^n \sigma_i g\left(\boldsymbol{x}_i,\boldsymbol{l}_i\right)\right],$$
$$\widetilde{\mathfrak{R}}_n\left(\mathcal{G}_{sp}^U\right) = \mathbb{E}_{\boldsymbol{x},\boldsymbol{l},\boldsymbol{\sigma}}\left[\sup_{g\in\mathcal{G}_{sp}^U}\sum_{i=1}^n \sigma_i g\left(\boldsymbol{x}_i,\boldsymbol{l}_i\right)\right],$$

where $\boldsymbol{\sigma} = \{\sigma_1, \sigma_2, \cdots, \sigma_n\}$ is n Rademacher variables with σ_i independently uniform variable taking value in $\{+1, -1\}$. Then we have:

Lemma A.1. *We suppose that the loss function $\mathcal{L}_{sp}^L = \sum_{j=1}^c 2\pi_j l_j\left(1 - f^j(\boldsymbol{x})\right)$ and $\mathcal{L}_{sp}^U = \sum_{j=1}^c \left(f^j(\boldsymbol{x}) - \pi_j\right)$ could be bounded by M, i.e., $M = \sup_{\boldsymbol{x}\in\mathcal{X}, f\in\mathcal{F}, \boldsymbol{l}\in\mathcal{Y}} \max(\mathcal{L}_{sp}^L(f(\boldsymbol{x}),\boldsymbol{l}), \mathcal{L}_{sp}^U(f(\boldsymbol{x}),\boldsymbol{l}))$, and for any $\delta > 0$, with probability at least $1-\delta$, we have:*

$$\sup_{f\in\mathcal{F}} |\mathcal{R}_{sp}^L(f) - \hat{\mathcal{R}}_{sp}^L(f)| \leq \frac{2}{C}\widetilde{\mathfrak{R}}_n\left(\mathcal{G}_{sp}^L\right) + \frac{M}{2\min_j |\mathcal{S}_{L_j}|}\sqrt{\frac{\log\frac{2}{\delta}}{2n}},$$
$$\sup_{f\in\mathcal{F}} |\mathcal{R}_{sp}^U(f) - \hat{\mathcal{R}}_{sp}^U(f)| \leq 2\widetilde{\mathfrak{R}}_n\left(\mathcal{G}_{sp}^U\right) + \frac{M}{2}\sqrt{\frac{\log\frac{2}{\delta}}{2n}},$$

where $\mathcal{R}_{sp}^L(f) = \sum_{j=1}^c 2\pi_j \mathbb{E}_{\boldsymbol{x}\sim p(\boldsymbol{x}|y_j=1)}\left[1 - f^j(\boldsymbol{x})\right]$, $\mathcal{R}_{sp}^U(f) = \mathbb{E}_{\boldsymbol{x}\sim p(\boldsymbol{x})}\sum_{j=1}^c \left[f^j(\boldsymbol{x})\right] - \pi_j$ and $C = \min_j \mathbb{E}_{\tilde{\mathcal{D}}}\left[\sum_{i=1}^n l_i^j\right]$ is a constant.

Proof. Suppose an example $(\boldsymbol{x}, \boldsymbol{l})$ is replaced by another arbitrary example $(\boldsymbol{x}', \boldsymbol{l}')$, then the change of $\sup_{f\in\mathcal{F}} \mathcal{R}_{sp}^L(f) - \hat{\mathcal{R}}_{sp}^L(f)$ is no greater than $\frac{M}{2n\min_j |\mathcal{S}_{L_j}|}$. By applying McDiarmid's inequality, for any $\delta > 0$, with probility at least $1 - \frac{\delta}{2}$,

$$\sup_{f\in\mathcal{F}} \mathcal{R}_{sp}^L(f) - \hat{\mathcal{R}}_{sp}^L(f) \leq \mathbb{E}\left[\sup_{f\in\mathcal{F}} \mathcal{R}_{sp}^L(f) - \hat{\mathcal{R}}_{sp}^L(f)\right] + \frac{M}{2\min_j |\mathcal{S}_{L_j}|}\sqrt{\frac{\log\frac{2}{\delta}}{2n}}.$$

By symmetry, we can obtain

$$\sup_{f\in\mathcal{F}} |\mathcal{R}_{sp}^L(f) - \hat{\mathcal{R}}_{sp}^L(f)| \leq \mathbb{E}\left[\sup_{f\in\mathcal{F}} \mathcal{R}_{sp}^L(f) - \hat{\mathcal{R}}_{sp}^L(f)\right] + \frac{M}{2\min_j |\mathcal{S}_{L_j}|}\sqrt{\frac{\log\frac{2}{\delta}}{2n}}.$$

Next is to bound the term $\mathbb{E}\left[\sup_{f\in\mathcal{F}}\mathcal{R}_{sp}^{L}(f)-\hat{\mathcal{R}}_{sp}^{L}(f)\right]$:

$$
\begin{aligned}
&\mathbb{E}\left[\sup_{f\in\mathcal{F}}\mathcal{R}_{sp}^{L}(f)-\hat{\mathcal{R}}_{sp}^{L}(f)\right]=\mathbb{E}_{\tilde{\mathcal{D}}}\left[\sup_{f\in\mathcal{F}}\mathcal{R}_{sp}^{L}(f)-\hat{\mathcal{R}}_{sp}^{L}(f)\right]\\
&=\mathbb{E}_{\tilde{\mathcal{D}}}\left[\sup_{f\in\mathcal{F}}\mathbb{E}_{\tilde{\mathcal{D}}'}\left[\hat{\mathcal{R}}_{sp}^{\prime L}(f)-\hat{\mathcal{R}}_{sp}^{L}(f)\right]\right]\\
&\leq\mathbb{E}_{\tilde{\mathcal{D}},\tilde{\mathcal{D}}'}\left[\sup_{f\in\mathcal{F}}\left[\hat{\mathcal{R}}_{sp}^{\prime L}(f)-\hat{\mathcal{R}}_{sp}^{L}(f)\right]\right]\\
&=\mathbb{E}_{\tilde{\mathcal{D}},\tilde{\mathcal{D}}',\boldsymbol{\sigma}}\left[\sup_{f\in\mathcal{F}}\sum_{i=1}^{n}\sum_{j=1}^{c}\sigma_i\left(\frac{2\pi_j}{\sum_{i=1}^{n}l_i^{\prime j}}l_i^{\prime j}\left(1-f^j(\boldsymbol{x}_i')\right)-\frac{2\pi_j}{\sum_{i=1}^{n}l_i^{j}}l_i^{j}\left(1-f^j(\boldsymbol{x}_i)\right)\right)\right]\\
&\leq\mathbb{E}_{\tilde{\mathcal{D}}',\boldsymbol{\sigma}}\left[\sup_{f\in\mathcal{F}}\sum_{i=1}^{n}\sum_{j=1}^{c}\sigma_i\left(\frac{2\pi_j}{\sum_{i=1}^{n}l_i^{\prime j}}l_i^{\prime j}\left(1-f^j(\boldsymbol{x}_i')\right)\right)\right]\\
&+\mathbb{E}_{\tilde{\mathcal{D}},\boldsymbol{\sigma}}\left[\sup_{f\in\mathcal{F}}\sum_{i=1}^{n}\sum_{j=1}^{c}\sigma_i\left(\frac{2\pi_j}{\sum_{i=1}^{n}l_i^{j}}l_i^{j}\left(1-f^j(\boldsymbol{x}_i)\right)\right)\right]\\
&\leq\frac{1}{C}\mathbb{E}_{\tilde{\mathcal{D}}',\boldsymbol{\sigma}}\left[\sup_{f\in\mathcal{F}}\sum_{i=1}^{n}\sum_{j=1}^{c}\sigma_i\left(2\pi_j l_i^{\prime j}\left(1-f^j(\boldsymbol{x}_i')\right)\right)\right]\\
&+\frac{1}{C}\mathbb{E}_{\tilde{\mathcal{D}},\boldsymbol{\sigma}}\left[\sup_{f\in\mathcal{F}}\sum_{i=1}^{n}\sum_{j=1}^{c}\sigma_i\left(2\pi_j l_i^{j}\left(1-f^j(\boldsymbol{x}_i)\right)\right)\right]\\
&=\frac{2}{C}\widetilde{\mathfrak{R}}_n\left(\mathcal{G}_{sp}^{L}\right),
\end{aligned}
$$

where C is a constant that $C=\min_j\mathbb{E}_{\tilde{\mathcal{D}}}\left[\sum_{i=1}^{n}y_i^j\right]$. Then we have:

$$
\sup_{f\in\mathcal{F}}|\mathcal{R}_{sp}^{L}(f)-\hat{\mathcal{R}}_{sp}^{L}(f)|\leq\frac{2}{C}\widetilde{\mathfrak{R}}_n\left(\mathcal{G}_{sp}^{L}\right)+\frac{M}{2\min_j|\mathcal{S}_{L_j}|}\sqrt{\frac{\log\frac{2}{\delta}}{2n}}.
$$

Similarly, we can obtain:

$$
\sup_{f\in\mathcal{F}}|\mathcal{R}_{sp}^{U}(f)-\hat{\mathcal{R}}_{sp}^{U}(f)|\leq2\widetilde{\mathfrak{R}}_n\left(\mathcal{G}_{sp}^{U}\right)+\frac{M}{2}\sqrt{\frac{\log\frac{2}{\delta}}{2n}},
$$

□

Lemma A.2. *Define* $\rho=\max_j 2\pi_j$, $\mathcal{H}_j=\left\{h:\boldsymbol{x}\mapsto f^j(\boldsymbol{x})|f\in\mathcal{F}\right\}$ *and* $\mathfrak{R}_n\left(\mathcal{H}_j\right)=\mathbb{E}_{p(\boldsymbol{x})}\mathbb{E}_{\boldsymbol{\sigma}}\left[\sup_{h\in\mathcal{H}_j}\frac{1}{n}\sum_{i=1}^{n}h\left(\boldsymbol{x}_i\right)\right]$. *Then, we have with Rademacher vector contraction inequality:*

$$
\widetilde{\mathfrak{R}}_n\left(\mathcal{G}_{sp}^{L}\right)\leq\sqrt{2}\rho\sum_{j=1}^{c}\mathfrak{R}_n(\mathcal{H}_j),\qquad\widetilde{\mathfrak{R}}_n\left(\mathcal{G}_{sp}^{U}\right)\leq\sqrt{2}\sum_{j=1}^{c}\mathfrak{R}_n(\mathcal{H}_j),
$$

Based on Lemma A.1 and Lemma A.2, we could obtain the following theorem.

Theorem A.3. *Assume the loss function* $\mathcal{L}_{sp}^{L}=\sum_{j=1}^{c}2\pi_j l_j\left(1-f^j(\boldsymbol{x})\right)$ *and* $\mathcal{L}_{sp}^{U}=\sum_{j=1}^{c}\left(f^j(\boldsymbol{x})-\pi_j\right)$ *could be bounded by* M, *i.e.,* $M=$

Table 6: Characteristics of the MLIC datasets.

Dataset	#Training	#Validation	#Testing	#Classes
VOC	4574	1143	5823	20
COCO	65665	16416	40137	80
NUS	120000	30000	60260	81
CUB	4795	1199	5794	312

Table 7: Characteristics of the MLL datasets.

Dataset	#Examples	#Features	#Classes	#Domain
Image	2000	294	5	Images
Scene	2407	294	6	Images
Yeast	2417	103	14	Biology
Corel5k	5000	499	374	Images
Mirflickr	24581	1000	38	Images
Delicious	16091	500	983	Text

$\sup_{\boldsymbol{x}\in\mathcal{X},f\in\mathcal{F},\boldsymbol{l}\in\mathcal{Y}} \max(\mathcal{L}_{sp}^{L}(f(\boldsymbol{x}),\boldsymbol{l}),\mathcal{L}_{sp}^{U}(f(\boldsymbol{x}),\boldsymbol{y}))$*, with probability at least* $1-\delta$*, we have:*

$$\begin{aligned}\mathcal{R}(\hat{f}_{sp})-\mathcal{R}(f^{\star}) &\leq \frac{4}{C}\sum_{j=1}^{c}\widetilde{\mathfrak{R}}_n\left(\mathcal{G}_{sp}^{L}\right)+\frac{M}{\min_j|\mathcal{S}_{L_j}|}\sqrt{\frac{\log\frac{4}{\delta}}{2n}}+4\widetilde{\mathfrak{R}}_n\left(\mathcal{G}_{sp}^{U}\right)+M\sqrt{\frac{\log\frac{4}{\delta}}{2n}}\\ &\leq \frac{4\sqrt{2}\rho}{C}\sum_{j=1}^{c}\mathfrak{R}_n(\mathcal{H}_j)+\frac{M}{\min_j|\mathcal{S}_{L_j}|}\sqrt{\frac{\log\frac{4}{\delta}}{2n}}+4\sqrt{2}\sum_{j=1}^{c}\mathfrak{R}_n(\mathcal{H}_j)+M\sqrt{\frac{\log\frac{4}{\delta}}{2n}}.\end{aligned}$$

Proof.

$$\begin{aligned}\mathcal{R}(\hat{f}_{sp})-\mathcal{R}(f^{\star}) &= \mathcal{R}(\hat{f}_{sp})-\hat{\mathcal{R}}_{sp}(\hat{f})+\hat{\mathcal{R}}_{sp}(\hat{f})-\hat{\mathcal{R}}_{sp}(f^{\star})+\hat{\mathcal{R}}_{sp}(f^{\star})-\mathcal{R}(f^{\star})\\ &\leq \mathcal{R}(\hat{f}_{sp})-\hat{\mathcal{R}}_{sp}(\hat{f})+\hat{\mathcal{R}}_{sp}(f^{\star})-\mathcal{R}(f^{\star})\\ &= \mathcal{R}_{sp}^{L}(\hat{f}_{sp})-\hat{\mathcal{R}}_{sp}^{L}(\hat{f})+\hat{\mathcal{R}}_{sp}^{L}(f^{\star})-\mathcal{R}_{sp}^{L}(f^{\star})\\ &+\mathcal{R}_{sp}^{U}(\hat{f}_{sp})-\hat{\mathcal{R}}_{sp}^{U}(\hat{f})+\hat{\mathcal{R}}_{sp}^{U}(f^{\star})-\mathcal{R}_{sp}^{U}(f^{\star})\\ &\leq 2\sup_{f\in\mathcal{F}}|\mathcal{R}_{sp}^{L}(f)-\hat{\mathcal{R}}_{sp}^{L}(f)|+2\sup_{f\in\mathcal{F}}|\mathcal{R}_{sp}^{U}(f)-\hat{\mathcal{R}}_{sp}^{U}(f)|\\ &\leq \frac{4}{C}\widetilde{\mathfrak{R}}_n\left(\mathcal{G}_{sp}^{L}\right)+\frac{M}{\min_j|\mathcal{S}_{L_j}|}\sqrt{\frac{\log\frac{4}{\delta}}{2n}}+4\widetilde{\mathfrak{R}}_n\left(\mathcal{G}_{sp}^{U}\right)+M\sqrt{\frac{\log\frac{4}{\delta}}{2n}}\\ &\leq \frac{4\sqrt{2}\rho}{C}\sum_{j=1}^{c}\mathfrak{R}_n(\mathcal{H}_j)+\frac{M}{\min_j|\mathcal{S}_{L_j}|}\sqrt{\frac{\log\frac{4}{\delta}}{2n}}+4\sqrt{2}\sum_{j=1}^{c}\mathfrak{R}_n(\mathcal{H}_j)+M\sqrt{\frac{\log\frac{4}{\delta}}{2n}}.\end{aligned}$$

□

A.6 Implementation Details

During the implementation, we first initialize the predictive network by performing warm-up training with AN solution, which could facilitate learning a fine network in the early stages. Furthermore, after each epoch, the class prior is reestimated via the trained model. The code implementation is based on PyTorch, and the experiments are conducted on GeForce RTX 3090 GPUs. The batch size is selected from $\{8, 16\}$ and the number of epochs is set to 10. The learning rate and weight decay are selected from $\{10^{-2}, 10^{-3}, 10^{-4}, 10^{-5}\}$ with a validation set. The hyperparameters δ and τ are all fixed as 0.01. All the comparing methods run 5 trials on each datasets. For fairness, we employed ResNet-50 as the backbone for all comparing methods.

Table 8: Predictive performance of each comparing method on MLL datasets in terms of *Average Precision* (mean ± std). The best performance is highlighted in bold (the larger the better).

	Image	Scene	Yeast	Corel5k	Mirflickr	Delicious
AN	0.534±0.061	0.580±0.104	0.531±0.079	0.217±0.003	0.615±0.004	0.317±0.002
AN-LS	0.574±0.037	0.631±0.072	0.538±0.044	0.230±0.002	0.587±0.006	0.261±0.006
WAN	0.576±0.041	0.661±0.033	0.698±0.017	0.241±0.002	0.621±0.004	0.315±0.000
EPR	0.539±0.028	0.597±0.062	0.710±0.008	0.214±0.001	0.628±0.003	0.314±0.000
ROLE	0.606±0.041	0.700±0.040	0.711±0.013	0.203±0.003	0.516±0.027	0.130±0.003
EM	0.486±0.031	0.549±0.103	0.642±0.029	0.294±0.002	0.614±0.003	0.293±0.001
EM-APL	0.467±0.026	0.448±0.049	0.654±0.040	0.275±0.003	0.589±0.007	0.311±0.001
SMILE	0.670±0.021	0.722±0.071	0.751±0.004	0.295±0.004	**0.629±0.003**	0.318±0.001
LL-R	0.605±0.058	0.714±0.035	0.658±0.006	0.268±0.002	0.625±0.001	0.296±0.004
LL-CP	0.595±0.031	0.735±0.028	0.700±0.000	0.259±0.004	0.621±0.007	0.251±0.007
LL-CT	0.600±0.012	0.669±0.052	0.629±0.007	0.258±0.004	0.619±0.004	0.253±0.004
CRISP	**0.749±0.037**	**0.795±0.031**	**0.758±0.002**	**0.304±0.003**	0.628±0.003	**0.319±0.001**

Table 9: Predictive performance of each comparing method on MLL datasets in terms of *Coverage* (mean ± std). The best performance is highlighted in bold (the smaller the better).

	Image	Scene	Yeast	Corel5k	Mirflickr	Delicious
AN	0.374±0.050	0.279±0.094	0.707±0.045	0.330±0.001	0.342±0.003	0.653±0.001
AN-LS	0.334±0.033	0.217±0.052	0.703±0.012	0.441±0.009	0.433±0.015	0.830±0.016
WAN	0.313±0.040	0.192±0.019	0.512±0.045	0.309±0.001	0.334±0.002	0.632±0.001
EPR	0.352±0.043	0.254±0.046	0.506±0.011	0.328±0.001	0.332±0.002	0.637±0.001
ROLE	0.306±0.049	0.157±0.023	0.519±0.026	0.551±0.007	0.448±0.028	0.887±0.004
EM	0.407±0.036	0.281±0.096	0.575±0.042	0.382±0.005	0.359±0.010	0.753±0.004
EM-APL	0.438±0.022	0.360±0.057	0.556±0.045	0.335±0.005	0.369±0.005	0.765±0.006
SMILE	0.242±0.014	0.146±0.037	0.462±0.003	0.308±0.007	0.328±0.004	0.628±0.003
LL-R	0.311±0.059	0.141±0.017	0.512±0.002	0.274±0.002	0.335±0.006	0.622±0.001
LL-CP	0.296±0.031	0.136±0.016	0.518±0.001	**0.272±0.008**	0.337±0.005	0.708±0.004
LL-CT	0.297±0.017	0.161±0.031	0.509±0.001	0.277±0.005	0.335±0.003	0.708±0.002
CRISP	**0.164±0.012**	**0.082±0.018**	**0.455±0.002**	0.276±0.002	**0.324±0.001**	**0.620±0.001**

Table 10: Predictive performance of each comparing methods on MLL datasets in terms of *Hamming loss* (mean ± std). The best performance is highlighted in bold (the smaller the better).

	Image	Scene	Yeast	Corel5k	Mirflickr	Delicious
AN	0.229±0.000	0.176±0.001	0.306±0.000	**0.010±0.000**	0.127±0.000	**0.019±0.000**
AN-LS	0.229±0.000	0.168±0.004	0.306±0.000	**0.010±0.000**	0.127±0.000	**0.019±0.000**
WAN	0.411±0.060	0.299±0.035	0.285±0.016	0.156±0.001	0.191±0.006	0.102±0.000
EPR	0.370±0.043	0.220±0.026	0.234±0.007	0.016±0.000	0.136±0.002	0.020±0.000
ROLE	0.256±0.018	0.176±0.017	0.279±0.010	**0.010±0.000**	0.128±0.000	**0.019±0.000**
EM	0.770±0.001	0.820±0.003	0.669±0.025	0.589±0.003	0.718±0.010	0.630±0.005
EM-APL	0.707±0.088	0.780±0.082	0.641±0.032	0.648±0.006	0.754±0.017	0.622±0.006
SMILE	0.219±0.009	0.182±0.021	**0.208±0.002**	**0.010±0.000**	0.127±0.001	0.081±0.008
LL-R	0.220±0.013	0.162±0.005	0.312±0.001	0.015±0.001	0.124±0.002	**0.019±0.000**
LL-CP	0.218±0.016	0.164±0.002	0.306±0.000	0.016±0.001	0.126±0.001	**0.019±0.000**
LL-CT	0.246±0.031	0.176±0.019	0.321±0.001	0.018±0.001	0.124±0.001	**0.019±0.000**
CRISP	**0.165±0.023**	**0.140±0.013**	0.211±0.001	**0.010±0.000**	**0.121±0.002**	**0.019±0.000**

A.7 Details of Datasets

The details of the four MLIC datasets and the five MLL datasets are provided in Table 6 and Table 7 respectively. The basic statics about the MLIC datasets include the number of training set, validation set, and testing set (#Training, #Validation, #Testing), and the number of classes (#Classes). The basic statics about the MLL datasets include the number of examples (#Examples), the dimension of features (#Features), the number of classes (#Classes), and the domain of the dataset (#Domain).

A.8 More Results of MLL Datasets

Table 8, 9, 10 and 11 report the results of our method and other comparing methods on five MLL datasets in terms of *Average Precision*, *Coverage, Hamming loss* and *One Error* respectively.

Table 11: Predictive performance of each comparing methods on MLL datasets in terms of *One-error* (mean ± std). The best performance is highlighted in bold (the smaller the better).

	Image	Scene	Yeast	Corel5k	Mirflickr	Delicious
AN	0.708±0.096	0.626±0.123	0.489±0.194	0.758±0.002	0.358±0.005	0.410±0.012
AN-LS	0.643±0.052	0.578±0.111	0.495±0.130	0.736±0.009	0.360±0.015	0.454±0.013
WAN	0.670±0.060	0.543±0.060	0.239±0.002	0.727±0.012	0.352±0.010	0.404±0.002
EPR	0.703±0.046	0.615±0.090	0.240±0.003	0.764±0.000	0.362±0.015	0.441±0.008
ROLE	0.605±0.041	0.507±0.066	0.244±0.005	0.705±0.016	0.525±0.072	0.594±0.006
EM	0.769±0.036	0.681±0.119	0.326±0.079	0.656±0.009	0.365±0.008	0.446±0.009
EM-APL	0.773±0.045	0.812±0.059	0.341±0.109	0.690±0.007	0.434±0.023	0.405±0.006
SMILE	0.533±0.036	0.466±0.117	0.250±0.012	0.650±0.008	0.340±0.010	**0.402±0.005**
LL-R	0.597±0.084	0.490±0.054	0.436±0.087	0.715±0.006	0.342±0.016	0.543±0.041
LL-CP	0.629±0.043	0.450±0.051	0.240±0.000	0.731±0.016	0.357±0.016	0.490±0.028
LL-CT	0.616±0.019	0.574±0.074	0.552±0.097	0.726±0.022	0.375±0.012	0.475±0.019
CRISP	**0.325±0.026**	**0.311±0.047**	**0.227±0.004**	**0.646±0.006**	**0.295±0.009**	**0.402±0.003**

Table 12: Summary of the Wilcoxon signed-ranks test for CRISP against other comparing approaches at 0.05 significance level. The *p*-values are shown in the brackets.

CRISP against	AN	AN-LS	WAN	EPR	ROLE	EM	EM-APL	SMILE	LL-R	LL-CP	LL-CT
Coverage	**win**[0.0313]	**win**[0.0313]	**win**[0.0313]	**win**[0.0313]	**win**[0.0313]	**win**[0.0313]	**win**[0.0313]	**win**[0.0313]	**win**[0.0431]	**win**[0.0431]	**win**[0.0431]
One-error	**win**[0.0313]	**win**[0.0313]	**win**[0.0313]	**win**[0.0313]	**win**[0.0313]	**win**[0.0313]	**win**[0.0313]	**win**[0.0431]	**tie**[0.625]	**win**[0.0313]	**win**[0.0313]
Ranking loss	**win**[0.0313]	**win**[0.0313]	**win**[0.0313]	**win**[0.0313]	**win**[0.0313]	**win**[0.0313]	**win**[0.0313]	**win**[0.0313]	**win**[0.0313]	**win**[0.0313]	**win**[0.0313]
Hamming loss	**tie**[0.0679]	**tie**[0.0679]	**win**[0.0313]	**win**[0.0313]	**tie**[0.0679]	**win**[0.0313]	**win**[0.0313]	**tie**[0.0796]	**win**[0.0313]	**win**[0.0313]	**win**[0.0313]
Average precision	**win**[0.0313]	**win**[0.0313]	**win**[0.0313]	**win**[0.0431]	**win**[0.0313]	**win**[0.0313]	**win**[0.0313]	**tie**[0.0938]	**win**[0.0313]	**win**[0.0313]	**win**[0.0313]

Table 13: Predictive performance of CRISP compared with the approach of estimating priors from the validation set (CRISP-VAL) on the MLL datasets for five metrics.

	Metrics	Image	Scene	Yeast	Corel5k	Mirflickr	Delicious
CRISP	*Coverage*	**0.164±0.012**	**0.082±0.018**	**0.455±0.002**	**0.276±0.002**	**0.324±0.001**	**0.620±0.001**
	Ranking Loss	**0.164±0.027**	**0.112±0.021**	**0.164±0.001**	**0.113±0.001**	**0.118±0.001**	**0.122±0.000**
	Average Precision	**0.749±0.037**	**0.795±0.031**	**0.758±0.002**	**0.304±0.003**	**0.628±0.003**	**0.319±0.001**
	Hamming Loss	**0.165±0.023**	**0.140±0.013**	**0.211±0.001**	**0.010±0.000**	**0.121±0.002**	**0.019±0.000**
	OneError	**0.325±0.026**	**0.311±0.047**	**0.227±0.004**	**0.646±0.006**	**0.295±0.009**	**0.402±0.003**
CRISP-VAL	*Coverage*	0.193±0.009	0.109±0.012	0.456±0.004	0.280±0.002	0.330±0.001	0.623±0.002
	Ranking Loss	0.198±0.016	0.116±0.013	0.165±0.001	0.114±0.002	0.120±0.001	**0.122±0.000**
	Average Precision	0.725±0.004	0.790±0.028	0.753±0.006	0.294±0.008	0.622±0.001	**0.319±0.001**
	Hamming Loss	0.180±0.006	0.141±0.014	0.216±0.000	**0.010±0.000**	0.124±0.001	**0.019±0.000**
	OneError	0.395±0.071	0.359±0.050	0.246±0.021	0.666±0.008	0.314±0.003	0.444±0.001

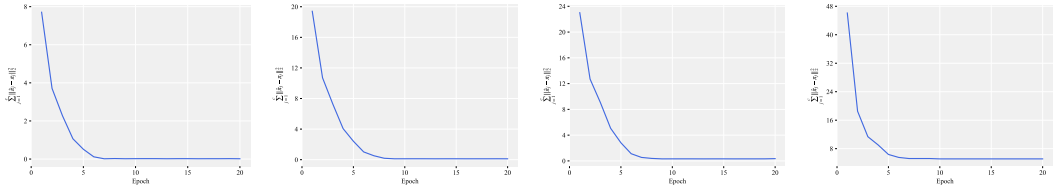

(a) VOC (b) COCO (c) NUS (d) CUB

Figure 4: Convergence of $\hat{\pi}$ on four MLIC datasets.

A.9 More Results of MLIC Datasets

Figure 4 illustrates the discrepancy between the estimated class-prior $\hat{\pi}_j$ and the true class-prior π_j in every epoch on four MLIC datasets. During the initial few epochs, a significant decrease in the discrepancy between the estimated class-prior and the true class-prior is observed. After several epochs, the estimated class prior tends to stabilize and converges to the true class-prior. This result provides evidence that our proposed method effectively estimates the class-prior with the only observed single positive label.

A.10 *p*-values of the wilcoxon signed-ranks test

Table 12 reports the *p*-values of the wilcoxon signed-ranks test [6] for the corresponding tests and the statistical test results at 0.05 significance level.

A.11 Ablation results of MLL datasets

Table 13 reports the predictive performance of CRISP compared with the approach of estimating priors from the validation set (CRISP-VAL) on the MLL datasets for five metrics. The results show that CRISP outperforms CRISP-VAL on almost all the five metrics.

NeurIPS Paper Checklist

1. **Claims**

   Question: Do the main claims made in the abstract and introduction accurately reflect the paper's contributions and scope?

   Answer: [Yes]

   Justification: See the abstract and the penultimate paragraph in introduction.

   Guidelines:

   - The answer NA means that the abstract and introduction do not include the claims made in the paper.
   - The abstract and/or introduction should clearly state the claims made, including the contributions made in the paper and important assumptions and limitations. A No or NA answer to this question will not be perceived well by the reviewers.
   - The claims made should match theoretical and experimental results, and reflect how much the results can be expected to generalize to other settings.
   - It is fine to include aspirational goals as motivation as long as it is clear that these goals are not attained by the paper.

2. **Limitations**

   Question: Does the paper discuss the limitations of the work performed by the authors?

   Answer: [Yes]

   Justification: We discussed the potential time complexity issues of the proposed algorithm in the Experiment Section 5.3.4.

   Guidelines:

   - The answer NA means that the paper has no limitation while the answer No means that the paper has limitations, but those are not discussed in the paper.
   - The authors are encouraged to create a separate "Limitations" section in their paper.
   - The paper should point out any strong assumptions and how robust the results are to violations of these assumptions (e.g., independence assumptions, noiseless settings, model well-specification, asymptotic approximations only holding locally). The authors should reflect on how these assumptions might be violated in practice and what the implications would be.
   - The authors should reflect on the scope of the claims made, e.g., if the approach was only tested on a few datasets or with a few runs. In general, empirical results often depend on implicit assumptions, which should be articulated.
   - The authors should reflect on the factors that influence the performance of the approach. For example, a facial recognition algorithm may perform poorly when image resolution is low or images are taken in low lighting. Or a speech-to-text system might not be used reliably to provide closed captions for online lectures because it fails to handle technical jargon.
   - The authors should discuss the computational efficiency of the proposed algorithms and how they scale with dataset size.
   - If applicable, the authors should discuss possible limitations of their approach to address problems of privacy and fairness.
   - While the authors might fear that complete honesty about limitations might be used by reviewers as grounds for rejection, a worse outcome might be that reviewers discover limitations that aren't acknowledged in the paper. The authors should use their best judgment and recognize that individual actions in favor of transparency play an important role in developing norms that preserve the integrity of the community. Reviewers will be specifically instructed to not penalize honesty concerning limitations.

3. **Theory assumptions and proofs**

   Question: For each theoretical result, does the paper provide the full set of assumptions and a complete (and correct) proof?

   Answer: [Yes]

Justification: In Theorem 4.1 and Theorem 4.2, we have comprehensively presented the corresponding assumptions and proofs.

Guidelines:

- The answer NA means that the paper does not include theoretical results.
- All the theorems, formulas, and proofs in the paper should be numbered and cross-referenced.
- All assumptions should be clearly stated or referenced in the statement of any theorems.
- The proofs can either appear in the main paper or the supplemental material, but if they appear in the supplemental material, the authors are encouraged to provide a short proof sketch to provide intuition.
- Inversely, any informal proof provided in the core of the paper should be complemented by formal proofs provided in appendix or supplemental material.
- Theorems and Lemmas that the proof relies upon should be properly referenced.

4. **Experimental result reproducibility**

   Question: Does the paper fully disclose all the information needed to reproduce the main experimental results of the paper to the extent that it affects the main claims and/or conclusions of the paper (regardless of whether the code and data are provided or not)?

   Answer: [Yes]

   Justification: See the Section A.6 in Appendix.

   Guidelines:

   - The answer NA means that the paper does not include experiments.
   - If the paper includes experiments, a No answer to this question will not be perceived well by the reviewers: Making the paper reproducible is important, regardless of whether the code and data are provided or not.
   - If the contribution is a dataset and/or model, the authors should describe the steps taken to make their results reproducible or verifiable.
   - Depending on the contribution, reproducibility can be accomplished in various ways. For example, if the contribution is a novel architecture, describing the architecture fully might suffice, or if the contribution is a specific model and empirical evaluation, it may be necessary to either make it possible for others to replicate the model with the same dataset, or provide access to the model. In general. releasing code and data is often one good way to accomplish this, but reproducibility can also be provided via detailed instructions for how to replicate the results, access to a hosted model (e.g., in the case of a large language model), releasing of a model checkpoint, or other means that are appropriate to the research performed.
   - While NeurIPS does not require releasing code, the conference does require all submissions to provide some reasonable avenue for reproducibility, which may depend on the nature of the contribution. For example
     (a) If the contribution is primarily a new algorithm, the paper should make it clear how to reproduce that algorithm.
     (b) If the contribution is primarily a new model architecture, the paper should describe the architecture clearly and fully.
     (c) If the contribution is a new model (e.g., a large language model), then there should either be a way to access this model for reproducing the results or a way to reproduce the model (e.g., with an open-source dataset or instructions for how to construct the dataset).
     (d) We recognize that reproducibility may be tricky in some cases, in which case authors are welcome to describe the particular way they provide for reproducibility. In the case of closed-source models, it may be that access to the model is limited in some way (e.g., to registered users), but it should be possible for other researchers to have some path to reproducing or verifying the results.

5. **Open access to data and code**

   Question: Does the paper provide open access to the data and code, with sufficient instructions to faithfully reproduce the main experimental results, as described in supplemental material?

Answer: [No]

Justification: The code is currently proprietary and not publicly available. However, we have provided detailed information necessary for replicating the experiments.

Guidelines:

- The answer NA means that paper does not include experiments requiring code.
- Please see the NeurIPS code and data submission guidelines (`https://nips.cc/public/guides/CodeSubmissionPolicy`) for more details.
- While we encourage the release of code and data, we understand that this might not be possible, so "No" is an acceptable answer. Papers cannot be rejected simply for not including code, unless this is central to the contribution (e.g., for a new open-source benchmark).
- The instructions should contain the exact command and environment needed to run to reproduce the results. See the NeurIPS code and data submission guidelines (`https://nips.cc/public/guides/CodeSubmissionPolicy`) for more details.
- The authors should provide instructions on data access and preparation, including how to access the raw data, preprocessed data, intermediate data, and generated data, etc.
- The authors should provide scripts to reproduce all experimental results for the new proposed method and baselines. If only a subset of experiments are reproducible, they should state which ones are omitted from the script and why.
- At submission time, to preserve anonymity, the authors should release anonymized versions (if applicable).
- Providing as much information as possible in supplemental material (appended to the paper) is recommended, but including URLs to data and code is permitted.

6. **Experimental setting/details**

   Question: Does the paper specify all the training and test details (e.g., data splits, hyperparameters, how they were chosen, type of optimizer, etc.) necessary to understand the results?

   Answer: [Yes]

   Justification: See the Experiment Section and Section A.6 in Appendix.

   Guidelines:

   - The answer NA means that the paper does not include experiments.
   - The experimental setting should be presented in the core of the paper to a level of detail that is necessary to appreciate the results and make sense of them.
   - The full details can be provided either with the code, in appendix, or as supplemental material.

7. **Experiment statistical significance**

   Question: Does the paper report error bars suitably and correctly defined or other appropriate information about the statistical significance of the experiments?

   Answer: [Yes]

   Justification: For each set of experiments, we conducted five trials. In Table 12, we also performed a significance analysis.

   Guidelines:

   - The answer NA means that the paper does not include experiments.
   - The authors should answer "Yes" if the results are accompanied by error bars, confidence intervals, or statistical significance tests, at least for the experiments that support the main claims of the paper.
   - The factors of variability that the error bars are capturing should be clearly stated (for example, train/test split, initialization, random drawing of some parameter, or overall run with given experimental conditions).
   - The method for calculating the error bars should be explained (closed form formula, call to a library function, bootstrap, etc.)
   - The assumptions made should be given (e.g., Normally distributed errors).

- It should be clear whether the error bar is the standard deviation or the standard error of the mean.
- It is OK to report 1-sigma error bars, but one should state it. The authors should preferably report a 2-sigma error bar than state that they have a 96% CI, if the hypothesis of Normality of errors is not verified.
- For asymmetric distributions, the authors should be careful not to show in tables or figures symmetric error bars that would yield results that are out of range (e.g. negative error rates).
- If error bars are reported in tables or plots, The authors should explain in the text how they were calculated and reference the corresponding figures or tables in the text.

8. **Experiments compute resources**

   Question: For each experiment, does the paper provide sufficient information on the computer resources (type of compute workers, memory, time of execution) needed to reproduce the experiments?

   Answer: [Yes]

   Justification: See the Experiment Section.

   Guidelines:

   - The answer NA means that the paper does not include experiments.
   - The paper should indicate the type of compute workers CPU or GPU, internal cluster, or cloud provider, including relevant memory and storage.
   - The paper should provide the amount of compute required for each of the individual experimental runs as well as estimate the total compute.
   - The paper should disclose whether the full research project required more compute than the experiments reported in the paper (e.g., preliminary or failed experiments that didn't make it into the paper).

9. **Code of ethics**

   Question: Does the research conducted in the paper conform, in every respect, with the NeurIPS Code of Ethics `https://neurips.cc/public/EthicsGuidelines`?

   Answer: [Yes]

   Justification: The research conducted in the paper conform, in every respect, with the NeurIPS Code of Ethics.

   Guidelines:

   - The answer NA means that the authors have not reviewed the NeurIPS Code of Ethics.
   - If the authors answer No, they should explain the special circumstances that require a deviation from the Code of Ethics.
   - The authors should make sure to preserve anonymity (e.g., if there is a special consideration due to laws or regulations in their jurisdiction).

10. **Broader impacts**

    Question: Does the paper discuss both potential positive societal impacts and negative societal impacts of the work performed?

    Answer: [Yes]

    Justification: See the Section Impact Statements in Appendix.

    Guidelines:

    - The answer NA means that there is no societal impact of the work performed.
    - If the authors answer NA or No, they should explain why their work has no societal impact or why the paper does not address societal impact.
    - Examples of negative societal impacts include potential malicious or unintended uses (e.g., disinformation, generating fake profiles, surveillance), fairness considerations (e.g., deployment of technologies that could make decisions that unfairly impact specific groups), privacy considerations, and security considerations.

- The conference expects that many papers will be foundational research and not tied to particular applications, let alone deployments. However, if there is a direct path to any negative applications, the authors should point it out. For example, it is legitimate to point out that an improvement in the quality of generative models could be used to generate deepfakes for disinformation. On the other hand, it is not needed to point out that a generic algorithm for optimizing neural networks could enable people to train models that generate Deepfakes faster.
- The authors should consider possible harms that could arise when the technology is being used as intended and functioning correctly, harms that could arise when the technology is being used as intended but gives incorrect results, and harms following from (intentional or unintentional) misuse of the technology.
- If there are negative societal impacts, the authors could also discuss possible mitigation strategies (e.g., gated release of models, providing defenses in addition to attacks, mechanisms for monitoring misuse, mechanisms to monitor how a system learns from feedback over time, improving the efficiency and accessibility of ML).

11. **Safeguards**

    Question: Does the paper describe safeguards that have been put in place for responsible release of data or models that have a high risk for misuse (e.g., pretrained language models, image generators, or scraped datasets)?

    Answer: [Yes]

    Justification: This paper does not directly release the model, and the training data used does not contain any sensitive content.

    Guidelines:

    - The answer NA means that the paper poses no such risks.
    - Released models that have a high risk for misuse or dual-use should be released with necessary safeguards to allow for controlled use of the model, for example by requiring that users adhere to usage guidelines or restrictions to access the model or implementing safety filters.
    - Datasets that have been scraped from the Internet could pose safety risks. The authors should describe how they avoided releasing unsafe images.
    - We recognize that providing effective safeguards is challenging, and many papers do not require this, but we encourage authors to take this into account and make a best faith effort.

12. **Licenses for existing assets**

    Question: Are the creators or original owners of assets (e.g., code, data, models), used in the paper, properly credited and are the license and terms of use explicitly mentioned and properly respected?

    Answer: [Yes]

    Justification: See the Experimtent Section.

    Guidelines:

    - The answer NA means that the paper does not use existing assets.
    - The authors should cite the original paper that produced the code package or dataset.
    - The authors should state which version of the asset is used and, if possible, include a URL.
    - The name of the license (e.g., CC-BY 4.0) should be included for each asset.
    - For scraped data from a particular source (e.g., website), the copyright and terms of service of that source should be provided.
    - If assets are released, the license, copyright information, and terms of use in the package should be provided. For popular datasets, `paperswithcode.com/datasets` has curated licenses for some datasets. Their licensing guide can help determine the license of a dataset.
    - For existing datasets that are re-packaged, both the original license and the license of the derived asset (if it has changed) should be provided.

- If this information is not available online, the authors are encouraged to reach out to the asset's creators.

13. **New assets**

    Question: Are new assets introduced in the paper well documented and is the documentation provided alongside the assets?

    Answer: [No]

    Justification: The paper does not release new assets.

    Guidelines:

    - The answer NA means that the paper does not release new assets.
    - Researchers should communicate the details of the dataset/code/model as part of their submissions via structured templates. This includes details about training, license, limitations, etc.
    - The paper should discuss whether and how consent was obtained from people whose asset is used.
    - At submission time, remember to anonymize your assets (if applicable). You can either create an anonymized URL or include an anonymized zip file.

14. **Crowdsourcing and research with human subjects**

    Question: For crowdsourcing experiments and research with human subjects, does the paper include the full text of instructions given to participants and screenshots, if applicable, as well as details about compensation (if any)?

    Answer: [NA]

    Justification: The paper does not involve crowdsourcing nor research with human subjects.

    Guidelines:

    - The answer NA means that the paper does not involve crowdsourcing nor research with human subjects.
    - Including this information in the supplemental material is fine, but if the main contribution of the paper involves human subjects, then as much detail as possible should be included in the main paper.
    - According to the NeurIPS Code of Ethics, workers involved in data collection, curation, or other labor should be paid at least the minimum wage in the country of the data collector.

15. **Institutional review board (IRB) approvals or equivalent for research with human subjects**

    Question: Does the paper describe potential risks incurred by study participants, whether such risks were disclosed to the subjects, and whether Institutional Review Board (IRB) approvals (or an equivalent approval/review based on the requirements of your country or institution) were obtained?

    Answer: [No]

    Justification: The paper does not involve crowdsourcing nor research with human subjects.

    Guidelines:

    - The answer NA means that the paper does not involve crowdsourcing nor research with human subjects.
    - Depending on the country in which research is conducted, IRB approval (or equivalent) may be required for any human subjects research. If you obtained IRB approval, you should clearly state this in the paper.
    - We recognize that the procedures for this may vary significantly between institutions and locations, and we expect authors to adhere to the NeurIPS Code of Ethics and the guidelines for their institution.
    - For initial submissions, do not include any information that would break anonymity (if applicable), such as the institution conducting the review.

16. **Declaration of LLM usage**

Question: Does the paper describe the usage of LLMs if it is an important, original, or non-standard component of the core methods in this research? Note that if the LLM is used only for writing, editing, or formatting purposes and does not impact the core methodology, scientific rigorousness, or originality of the research, declaration is not required.

Answer: [NA]

Justification: The core method development in this research does not involve LLMs as any important, original, or non-standard components.

Guidelines:

- The answer NA means that the core method development in this research does not involve LLMs as any important, original, or non-standard components.
- Please refer to our LLM policy (`https://neurips.cc/Conferences/2025/LLM`) for what should or should not be described.